



LUND UNIVERSITY

Truck Model for Yaw Dynamics Control

Gäfvert, Magnus; Sanfridsson, Martin; Claesson, Vilgot

2000

Document Version:

Publisher's PDF, also known as Version of record

[Link to publication](#)

Citation for published version (APA):

Gäfvert, M., Sanfridsson, M., & Claesson, V. (2000). *Truck Model for Yaw Dynamics Control*. (Technical Reports TFRT-7588). Department of Automatic Control, Lund Institute of Technology (LTH).

Total number of authors:

3

General rights

Unless other specific re-use rights are stated the following general rights apply:

Copyright and moral rights for the publications made accessible in the public portal are retained by the authors and/or other copyright owners and it is a condition of accessing publications that users recognise and abide by the legal requirements associated with these rights.

- Users may download and print one copy of any publication from the public portal for the purpose of private study or research.
- You may not further distribute the material or use it for any profit-making activity or commercial gain
- You may freely distribute the URL identifying the publication in the public portal

Read more about Creative commons licenses: <https://creativecommons.org/licenses/>

Take down policy

If you believe that this document breaches copyright please contact us providing details, and we will remove access to the work immediately and investigate your claim.

LUND UNIVERSITY

PO Box 117
221 00 Lund
+46 46-222 00 00

ISSN 0280-5316
ISRN LUTFD2/TFRT--7588--SE

DICOSMOS INTERNAL REPORT

Revision 1.1

Truck Model for Yaw Dynamics Control

Magnus Gäfvert
Martin Sanfridson¹, Vilgot Claesson²

¹Mechatronics Lab
Royal Institute of Technology, Sweden

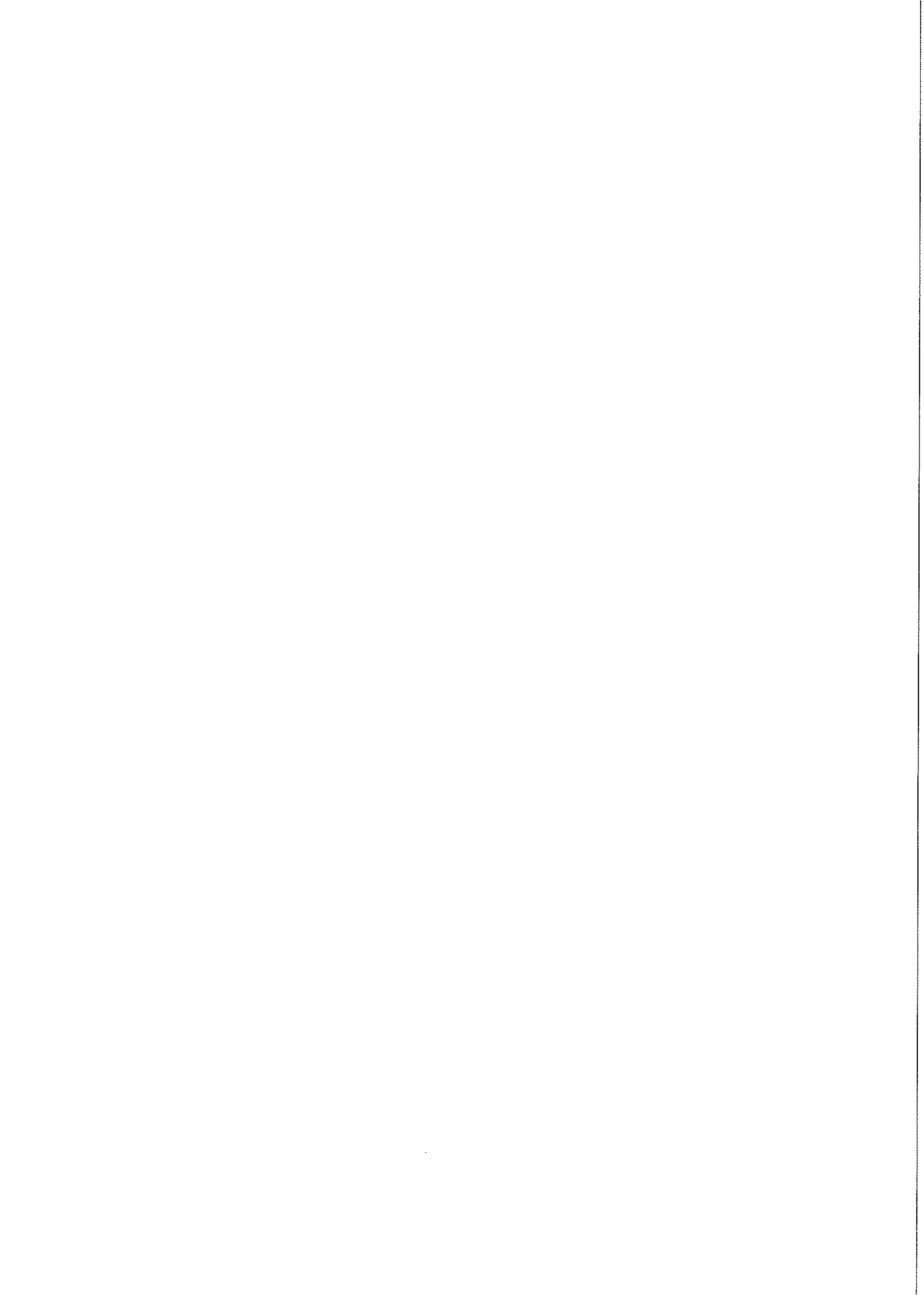
²Department of Computer Engineering
Chalmers Technical University, Sweden

Department of Automatic Control
Lund Institute of Technology, Sweden

September 2000

Department of Automatic Control Lund Institute of Technology Box 118 SE-221 00 Lund Sweden		<i>Document name</i> INTERNAL REPORT	
		<i>Date of issue</i> September 2000	
		<i>Document Number</i> ISRN LUTFD2/TFRT--7588-SE	
<i>Author(s)</i> Magnus Gäfvert., Martin Sanfridson., Vilgot Claesson		<i>Supervisor</i>	
		<i>Sponsoring organization</i>	
<i>Title and subtitle</i> Truck Model for Yaw Dynamics Control (Lastbilsmodell för reglering av girdynamik)			
<i>Abstract</i> <p>This report describes the derivation of a nonlinear model of a tractor-semitrailer combination vehicle. The purpose of the model is validation of yaw-control algorithms. The model includes 4 DOF in lateral, longitudinal, and yaw motion. It is formulated as a state space model with 5 state variables. Additional states are added with the rotational dynamics of the wheels. The model includes a static description of load-transfer, and a fairly detailed tyre model. A linearized version of the model is also presented. The nonlinear model is implemented in Simulink. Validation is performed by comparison with a multibody model. Examples of simulation outputs are presented.</p>			
<i>Keywords</i>			
<i>Classification system and/or index terms (if any)</i>			
<i>Supplementary bibliographical information</i>			
<i>ISSN and key title</i> 0280-5316			<i>ISBN</i>
<i>Language</i> English	<i>Number of pages</i> 45	<i>Recipient's notes</i>	
<i>Security classification</i>			

The report may be ordered from the Department of Automatic Control or borrowed through:
 University Library 2, Box 3, SE-221 00 Lund, Sweden
 Fax +46 46 222 44 22 E-mail ub2@ub2.se



Contents

1. Introduction	3
2. Extended Bicycle Model	3
2.1 Equations of Motion for a Rigid Vehicle	3
2.2 Equations of Motion for an Articulated Vehicle	5
3. Load Distribution and Load Transfer	9
3.1 Static Load Distribution	9
3.2 Longitudinal Load Transfer	10
3.3 Lateral Load Transfer	11
3.4 Normal Forces	12
4. Wheel Forces and Dynamics	12
5. Tire Model	12
6. Brake Model	14
7. Linear Semi-trailer Vehicle Model	16
7.1 Linearized Equations of Motion	17
7.2 Linear Tire Model	18
7.3 Complete Linear Vehicle Model	19
8. Simulink Model	21
8.1 Simulation Example	21
9. Validation	22
9.1 The Multi-body Simulation Model	22
9.2 Comparisons	23
Acknowledgements	27
10. References	27
A. Simulation Example Plots	29
B. Simulink Model Source	35
Matlab S-function	35
Tire Model	41

1. Introduction

In this report a nonlinear model for a semi-trailer combination vehicle is derived. The model is aimed at simulations of handling scenarios with active yaw control, using distributed braking and possibly tractor rear wheel steering. The model describes lateral, longitudinal, and yaw motion of the vehicle, as well as load transfer due to lateral and longitudinal acceleration. It also includes a fairly detailed model of tire-road contact forces. (An extension of the model includes roll dynamics.) Similar models are presented in [Ell69, Leu70, Ell94, CT00]. The model consists of two unsprung masses, and six wheels. Tire-road contact forces are described with a nonlinear tire model for combined cornering and braking. A Matlab/Simulink implementation of the model is used for handling simulations. Validation of the model is performed by comparisons with simulation results from a multibody model of similar complexity. A linear version of the model for use in controller synthesis is also derived.

2. Extended Bicycle Model

In this section an extended bicycle model [Mit90] is constructed. Equations describing planar and yaw motion for the tractor and semi-trailer combination are derived.

The derivation of the equations of motion will be carried out in the spirit of [Ell94]. The analytical background is described in detail in [FC93].

The vehicle equations of motions are most conveniently expressed in a vehicle fixed reference system. As a first step the equations of motion for a rigid vehicle, expressed in vehicle fixed coordinates, is derived. No notational distinction is made between scalar and vector variables in order not to clutter the the equations excessively. Similarly, some vector variables denote the representation of the vector in a certain coordinate system. The interpretation of the variables should be clear from the context.

2.1 Equations of Motion for a Rigid Vehicle

In the derivation of the equations of motion for the vehicle it is necessary to have an expression for the acceleration of arbitrary points on the vehicle body.

Motion of a point in vehicle coordinates Denote with '*' the earth fixed inertial reference frame, and with 'O' the vehicle fixed non-inertial reference frame rotating with the angular velocity ω and translating with the velocity v_O , see Figure 1. For any vector Q it holds that

$$\left(\frac{d}{dt}\right)_* Q = \left(\frac{d}{dt}\right)_O Q + \omega \times Q \quad (1)$$

In particular the velocity of P with respect to $*$ is expressed as the sum of the translational velocity of the vehicle reference system, and the time derivative of the position vector for P , r_P :

$$v_P = v_O + \left(\frac{d}{dt}\right)_* r_P = v_O + \left(\frac{d}{dt}\right)_O r_P + \omega \times r_P = v_O + \omega \times r_P \quad (2)$$

It is used that r_P is constant in the vehicle fixed reference frame, so that $(d/dt)_O r_P \equiv 0$. The acceleration of P is computed by applying (1) on (2):

$$\begin{aligned} a_P &= \left(\frac{d}{dt}\right)_* v_P = \left(\frac{d}{dt}\right)_O (v_O + \omega \times r_P) + \omega \times (v_O + \omega \times r_P) \\ &= \left(\left(\frac{d}{dt}\right)_O \omega\right) \times r_P + \left(\frac{d}{dt}\right)_O v_O + \omega \times (\omega \times r_P) + \omega \times v_O \quad (3) \end{aligned}$$

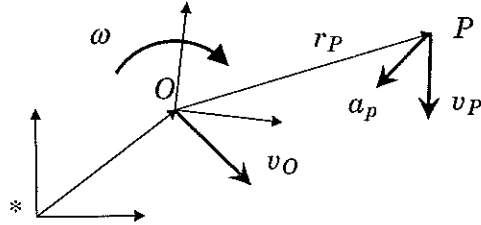


Figure 1 Acceleration of a particle in a rotating and translating reference frame.

Scalar expressions are achieved by introducing $r_P = xe_x^O + ye_y^O$, $v_O = Ue_x^O + Ve_y^O$ and $\omega = re_z^O$. Then

$$v_P = (U - ry) e_x^O + (V + rx) e_y^O \quad (4)$$

and

$$a_P = (\dot{U} - \dot{r}y - r^2x - rV) e_x^O + (\dot{V} + \dot{r}x - r^2y + rU) e_y^O \quad (5)$$

Equations of motion for the vehicle in local coordinates Now regard a rigid body \mathcal{B} (the vehicle) with mass m and center of mass CM located at $r_{CM} = \bar{x}e_x^O + \bar{y}e_y^O$, under influence of the external force F and the external moment N_O around O . The momentum p is

$$p = \int_{\mathcal{B}} dm_P v_P = m v_{CM}$$

Newton's second law states that

$$\left(\frac{d}{dt}\right)_* p = F$$

Thus

$$m \left(\frac{d}{dt}\right)_* v_{CM} = F$$

and with (5) inserted this yields

$$m \left((\dot{U} - \dot{r}\bar{y} - r^2\bar{x} - rV) e_x^O + (\dot{V} + \dot{r}\bar{x} - r^2\bar{y} + rU) e_y^O \right) = F$$

The angular momentum L_O around O is

$$L_O = \int_{\mathcal{B}} r_P \times dm_P v_P$$

Euler's equation of motion states that

$$\left(\frac{d}{dt}\right)_* L_O = N_0 \quad (6)$$

and using (1) and (2)

$$\begin{aligned} \left(\frac{d}{dt}\right)_* L_O &= \left(\frac{d}{dt}\right)_O L_O + \omega \times L_O = \int_{\mathcal{B}} r_P \times dm_P \left(\frac{d}{dt}\right)_O v_P = \\ &= \int_{\mathcal{B}} r_P \times dm_P \left(\frac{d}{dt}\right)_O (v_O + \omega \times r_P) = \\ &= \int_{\mathcal{B}} r_P \times dm_P \left(\left(\frac{d}{dt}\right)_O v_O + \left(\left(\frac{d}{dt}\right)_O \omega\right) \times r_P \right) = \\ &= \int_{\mathcal{B}} (x e_x^O + y e_y^O) \times dm_P \left((\dot{U} e_x^O + \dot{V} e_y^O) + \dot{r} e_z^O \times (x e_x^O + y e_y^O) \right) = \\ &= \int_{\mathcal{B}} (x^2 + y^2) dm_P \dot{r} e_z^O + m \bar{x} \dot{V} e_z^O - m \bar{y} \dot{U} e_z^O = I_O \dot{r} e_z^O + m \bar{x} \dot{V} e_z^O - m \bar{y} \dot{U} e_z^O \end{aligned} \quad (7)$$

where I_O is the moment of inertia of \mathcal{B} with respect to O .

With $F = X e_x^O + Y e_y^O$ and $N_0 = Z e_z^O$ the resulting scalar equations of motion are

$$\begin{aligned} m(\dot{U} - \dot{r}\bar{y} - r^2\dot{\bar{x}} - rV) &= X \\ m(\dot{V} + \dot{r}\bar{x} - r^2\dot{\bar{y}} + rU) &= Y \\ I_O \dot{r} + m\bar{x}(\dot{V} + Ur) - m\bar{y}(\dot{U} - Vr) &= Z \end{aligned} \quad (8)$$

2.2 Equations of Motion for an Articulated Vehicle

Introduce the articulated semi-trailer vehicle combination in Figure 2. Denote with '1' the tractor fixed reference system, and with '2' the semi-trailer fixed system. The origins of both systems are located in the fifth wheel. The articulation angle is denoted by ' ψ '. The representation of any vector q in the systems 1 and 2 is related by the rotational transformation

$$q_2 = Rq_1, \quad \text{with} \quad R = \begin{pmatrix} \cos \psi & \sin \psi & 0 \\ -\sin \psi & \cos \psi & 0 \\ 0 & 0 & 1 \end{pmatrix} \quad (9)$$

The vehicle combination is influenced by the tire contact forces $X_1, Y_1, X_2, Y_2, X_3, Y_3, X_4, Y_4, X_5, Y_5, X_6, Y_6$, and the internal reaction forces in the fifth wheel X_p, Y_p , as in Figure 3. Introduce the shorthand writing

$$\begin{aligned} \bar{X}_1 &= X_1 + X_2 + X_3 + X_4 \\ \bar{Y}_1 &= Y_1 + Y_2 + Y_3 + Y_4 \\ \bar{Z}_1 &= y_f X_1 + a_1 Y_1 - y_f X_2 + a_1 Y_2 + y_r X_3 - b_1 Y_3 - y_r X_4 - b_1 Y_4 \\ \bar{X}_2 &= X_5 + X_6 \\ \bar{Y}_2 &= Y_5 + Y_6 \\ \bar{Z}_2 &= y_t X_5 - b_2 Y_5 - y_t X_6 - b_2 Y_6 \end{aligned} \quad (10)$$

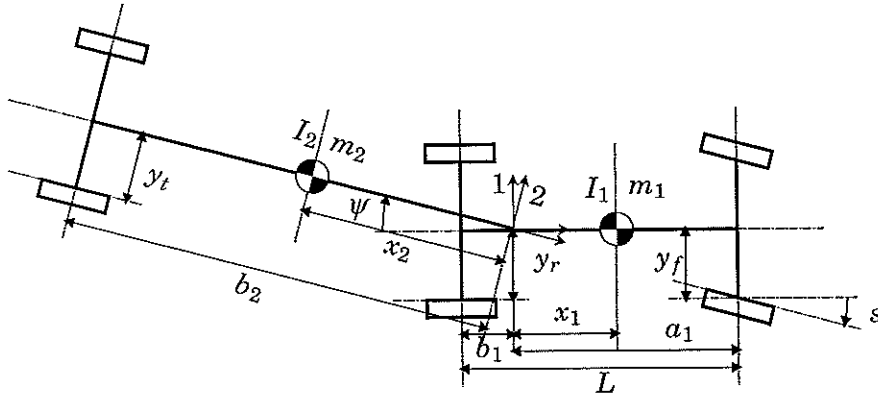


Figure 2 Geometry of the semi-trailer vehicle combination.

According to (8) the equations of motions for the tractor and semi-trailer

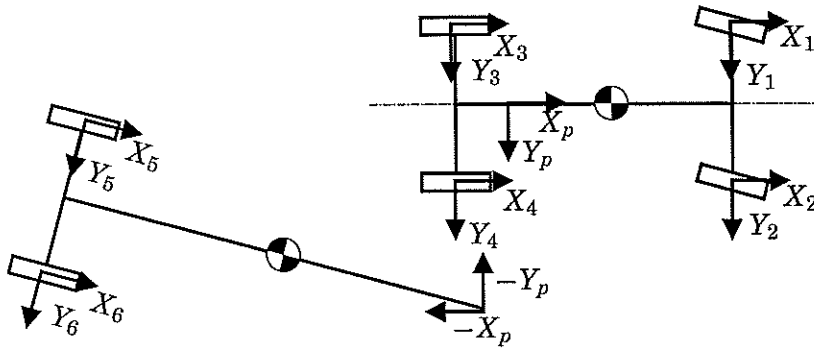


Figure 3 Forces acting on the semi-trailer vehicle combination.

are

$$\begin{aligned}
 m_1 (\dot{U}_1 - r_1^2 x_1 - r_1 V_1) &= \bar{X}_1 + X_p \\
 m_1 (\dot{V}_1 + r_1 x_1 + r_1 U_1) &= \bar{Y}_1 + Y_p \\
 I_1 \dot{r}_1 + m_1 x_1 (\dot{V}_1 + U_1 r_1) &= \bar{Z}_1 \\
 m_2 (\dot{U}_2 + r_2^2 x_2 - r_2 V_2) &= \bar{X}_2 - X_p \cos \psi - Y_p \sin \psi \\
 m_2 (\dot{V}_2 - r_2 x_2 + r_2 U_2) &= Y_2 + X_p \sin \psi - Y_p \cos \psi \\
 I_2 \dot{r}_2 - m_2 x_2 (\dot{V}_2 + U_2 r_2) &= \bar{Z}_2
 \end{aligned} \tag{11}$$

The CMs are assumed to be located such that $\bar{y} = 0$, and the different signs in the semi-trailer equations are due to the location of the semi-trailer CM behind the origin in the fifth wheel.

Elimination of semi-trailer variables The motions of the tractor and the semi-trailer are kinematically constrained by the fifth wheel, which enables elimination of \dot{U}_2 , \dot{V}_2 , U_2 , V_2 , and r_2 . The velocity of the origins of the reference systems is v , with the representations $v_1 = U_1 e_x^1 + V_1 e_y^1$ and $v_2 = U_2 e_x^2 + V_2 e_y^2$ respectively. The velocity vector representations are

related by the rotational transformation as $v_2 = Rv_1$. Thus

$$\begin{aligned} U_2 &= U_1 \cos \psi + V_1 \sin \psi \\ V_2 &= -U_1 \sin \psi + V_1 \cos \psi \end{aligned} \quad (12)$$

In the following, let $\omega_1 = r_1 e_z^1$ and $\omega_2 = r_2 e_z^2$ denote the angular velocities of the tractor and semi-trailer.

Then ω_1 and ω_2 are related to the articulation angle ψ as

$$\omega_2 - \omega_1 = \dot{\psi} e_z^{1,2} \quad (13)$$

or

$$\dot{\psi} = r_2 - r_1 \quad (14)$$

hence

$$\dot{r}_2 e_z^{1,2} - \dot{r}_1 e_z^{1,2} = \ddot{\psi} e_z^{1,2} \quad (15)$$

and

$$\dot{r}_2 - \dot{r}_1 = \ddot{\psi} \quad (16)$$

The acceleration at the fifth wheel can be expressed in the tractor or the semi-trailer systems, and are related by (1) as

$$\left(\frac{d}{dt} \right)_2 v + \omega_2 \times v = \left(\frac{d}{dt} \right)_1 v + \omega_1 \times v \quad (17)$$

With local representations

$$\left(\frac{d}{dt} \right)_2 v_2 = \left(\frac{d}{dt} \right)_1 v_1 + (r_1 - r_2) e_z^1 \times v_1 \quad (18)$$

which may be expanded to

$$\dot{U}_2 e_x^2 + \dot{V}_2 e_y^2 = (\dot{U}_1 + \dot{\psi} V_1) e_x^1 + (\dot{V}_1 - \dot{\psi} U_1) e_y^1 \quad (19)$$

Using the rotational transformation (9) this yields

$$\begin{aligned} \dot{U}_2 e_x^2 + \dot{V}_2 e_y^2 &= \left((\dot{U}_1 + \dot{\psi} V_1) \cos \psi + (\dot{V}_1 - \dot{\psi} U_1) \sin \psi \right) e_x^2 + \\ &\quad \left(-(\dot{U}_1 + \dot{\psi} V_1) \sin \psi + (\dot{V}_1 - \dot{\psi} U_1) \cos \psi \right) e_y^2 \end{aligned} \quad (20)$$

Thus

$$\begin{aligned} \dot{U}_2 &= (\dot{U}_1 + V_1 \dot{\psi}) \cos \psi + (\dot{V}_1 - U_1 \dot{\psi}) \sin \psi \\ \dot{V}_2 &= -(\dot{U}_1 + V_1 \dot{\psi}) \sin \psi + (\dot{V}_1 - U_1 \dot{\psi}) \cos \psi \end{aligned} \quad (21)$$

Insertion of (21) and (16) in (11) yields the equations of motion

$$m_1 (\dot{U}_1 - r_1^2 x_1 - r_1 V_1) = \ddot{X}_1 + X_p \quad (22a)$$

$$m_1 (\dot{V}_1 + \dot{r}_1 x_1 + r_1 U_1) = \bar{Y}_1 + Y_p \quad (22b)$$

$$I_1 \dot{r}_1 + m_1 x_1 (\dot{V}_1 + U_1 r_1) = \bar{Z}_1 \quad (22c)$$

$$m_2 \left((\dot{U}_1 - V_1 r_1) \cos \psi + (\dot{V}_1 + U_1 r_1) \sin \psi + (r_1 + \dot{\psi})^2 x_2 \right) = \bar{X}_2 - X_p \cos \psi - Y_p \sin \psi \quad (22d)$$

$$m_2 \left((\dot{V}_1 + U_1 r_1) \cos \psi - (\dot{U}_1 - V_1 r_1) \sin \psi - (\dot{r}_1 + \dot{\psi}) x_2 \right) = \bar{Y}_2 + X_p \sin \psi - Y_p \cos \psi \quad (22e)$$

$$I_2 (\dot{r}_1 + \dot{\psi}) - m_2 x_2 \left((\dot{V}_1 + U_1 r_1) \cos \psi - (\dot{U}_1 - V_1 r_1) \sin \psi \right) = \bar{Z}_2 \quad (22f)$$

Elimination of internal forces The internal forces X_p and Y_p may now be eliminated by combining the above equations as (22d) $\sin \psi$ + (22e) $\cos \psi$, yielding

$$m_2 \left(\dot{V}_1 + U_1 r_1 + (r_1 + \dot{\psi})^2 \bar{x}_2 \sin \psi - (\dot{r}_1 + \dot{\psi}) \bar{x}_2 \cos \psi \right) = \bar{X}_2 \sin \psi + \bar{Y}_2 \cos \psi - Y_p \quad (22g)$$

and (22d) $\cos \psi$ - (22e) $\sin \psi$, yielding

$$m_2 \left(\dot{U}_1 - V_1 r_1 + (r_1 + \dot{\psi})^2 \bar{x}_2 \cos \psi + (\dot{r}_1 + \dot{\psi}) \bar{x}_2 \sin \psi \right) = \bar{X}_2 \cos \psi - \bar{Y}_2 \sin \psi - X_p \quad (22h)$$

Now (22a)+(22h), (22b)+(22g), (22c) and (22f) give the reduced equations of motion

$$\begin{aligned} (m_1 + m_2) (\dot{U}_1 - V_1 r_1) - m_1 r_1^2 x_1 + m_2 (r_1 + \dot{\psi})^2 x_2 \cos \psi + \\ m_2 (\dot{r}_1 + \dot{\psi}) x_2 \sin \psi &= \bar{X}_1 + \bar{X}_2 \cos \psi - \bar{Y}_2 \sin \psi \\ (m_1 + m_2) (\dot{V}_1 + U_1 r_1) + m_1 \dot{r}_1 x_1 + m_2 (r_1 + \dot{\psi})^2 x_2 \sin \psi - \\ m_2 (\dot{r}_1 + \dot{\psi}) x_2 \cos \psi &= \bar{Y}_1 + \bar{X}_2 \sin \psi + \bar{Y}_2 \cos \psi \\ I_1 \dot{r}_1 + m_1 x_1 (\dot{V}_1 + U_1 r_1) &= \bar{Z}_1 \end{aligned} \quad (23)$$

$$I_2 (\dot{r}_1 + \dot{\psi}) - m_2 x_2 \left((\dot{V}_1 + U_1 r_1) \cos \psi - (\dot{U}_1 - V_1 r_1) \sin \psi \right) = \bar{Z}_2$$

With the introduction of the state vector

$$\xi' = (U, V, r, \dot{\psi}, \psi)^T \quad (24)$$

these equations are conveniently written on matrix form as

$$H(\xi') \frac{d\xi'}{dt} = F(\xi', \bar{X}_1, \bar{X}_2, \bar{Y}_1, \bar{Y}_2, \bar{Z}_1, \bar{Z}_2) \quad (25)$$

with

$$H(\xi') = \begin{pmatrix} m & 0 & m_2 x_2 \sin \psi & m_2 x_2 \sin \psi & 0 \\ 0 & m & m_1 x_1 - m_2 x_2 \cos \psi & -m_2 x_2 \cos \psi & 0 \\ 0 & m_1 x_1 & I_1 & 0 & 0 \\ m_2 x_2 \sin \psi & -m_2 x_2 \cos \psi & I_2 & I_2 & 0 \\ 0 & 0 & 0 & 0 & 1 \end{pmatrix} \quad (26)$$

and

$$F(\xi, \bar{X}_1, \bar{X}_2, \bar{Y}_1, \bar{Y}_2, \bar{Z}_1, \bar{Z}_2) = \begin{pmatrix} mVr + m_1r^2x_1 - m_2(r + \dot{\psi})^2x_2 \cos \psi + \bar{X}_1 + \bar{X}_2 \cos \psi - \bar{Y}_2 \sin \psi \\ -mUr - m_2(r + \dot{\psi})^2\bar{x}_2 \sin \psi + \bar{Y}_1 + \bar{X}_2 \sin \psi + \bar{Y}_2 \cos \psi \\ -m_1x_1Ur\bar{Z}_1 \\ m_2x_2r(U \cos \psi + V \sin \psi) + \bar{Z}_2 \\ \dot{\psi} \end{pmatrix} \quad (27)$$

where $m = m_1 + m_2$, and the indices on U , V and r has been dropped. This is a suitable form for numerical integration, where the left hand matrix has to be inverted in each simulation step.

3. Load Distribution and Load Transfer

The normal force a tire apply on the road greatly influences the lateral and longitudinal forces that the tire can carry. Therefore it is essential to model how the normal forces vary with vehicle geometry and driving conditions. The changing normal forces affect the road/tire contact forces, and thus have influence on the handling characteristics of the vehicle combination at certain maneuvers. A crude model of this behaviour is described in this section.

The normal force distribution at rest only depends on the vehicle geometry. This is denoted the *static load distribution*. For heavy vehicles inertial forces due to lateral and longitudinal accelerations result in fairly large pitch and roll moments, because of the height of the center of mass. These moments are carried by the normal forces of the tires, and thus result in normal forces that deviates from the static load distribution. Denote these normal force variations by *load transfer*.

In reality the load transfer depends much on suspension and chassis stiffness, and the roll and pitch behaviour of the vehicle. Since neither roll nor pitch movements are included in the model in this report, the load distribution and load transfer are modeled based on simple static assumptions. The static load distribution is derived in Section 3.1 below, while the load transfer due to inertial forces is derived in Sections 3.2–3.3.

3.1 Static Load Distribution

It is assumed that wheels mounted on the same axle carry equal load at rest (symmetry assumption). The lumped normal forces are denoted by N_f , N_r and N_t . The fifth wheel normal force is denoted by N_O . See Figure 4. From the normal force balance

$$N_t + N_O = m_2g$$

and the balance of moments around the fifth wheel

$$N_t b_2 = m_2 g x_2$$

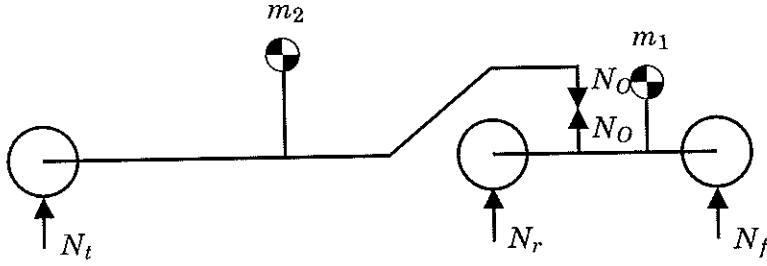


Figure 4 Static load transfer model.

the semi-trailer rear axle normal force N_t and the fifth wheel normal force N_O are resolved as

$$N_t = m_2 g x_2 / b_2 \quad (28)$$

$$N_O = m_2 g (b_2 - x_2) / b_2 \quad (29)$$

In the same manner the tractor force balance

$$N_r + N_f = m_1 g + N_O$$

and the tractor balance of moments around the front axle

$$N_r (b_1 + a_1) - N_O a_1 = m_1 g (a_1 - x_1)$$

gives the tractor front and rear axle normal forces as

$$N_r = (N_O a_1 + m_1 g (a_1 - x_1)) / (b_1 + a_1) \quad (30)$$

$$N_f = (m_1 g (b_1 + x_1) + N_O b_1) / (b_1 + a_1) \quad (31)$$

3.2 Longitudinal Load Transfer

The longitudinal load transfer is computed by lumping the wheels on the same axles, as in Figure 5. The lumped longitudinal load transfer forces

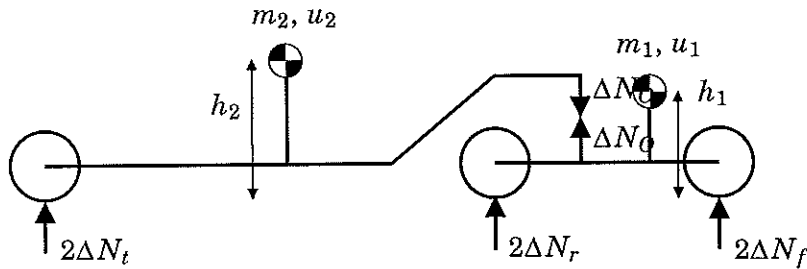


Figure 5 Static load transfer model.

are denoted ΔN_f , ΔN_r and ΔN_t . The fifth wheel longitudinal load transfer force is denoted by ΔN_O . The tractor and semi-trailer CM longitudinal accelerations are denoted by \dot{u}_1 and \dot{u}_2 respectively. From the semi-trailer normal force balance

$$2\Delta N_t + \Delta N_O = 0$$

and the balance of moments around the fifth wheel

$$2\Delta N_t b_2 - m_2 \dot{u}_2 h_2 = 0$$

the semi-trailer rear axle normal force ΔN_t and the fifth wheel normal force ΔN_O are resolved as

$$\Delta N_t = m_2 \dot{u}_2 h_2 / 2b_2 \quad (32)$$

$$\Delta N_O = -m_2 \dot{u}_2 h_2 / b_2 \quad (33)$$

In the same manner the tractor force balance

$$2\Delta N_r + 2\Delta N_f = \Delta N_O$$

and the tractor balance of moments around the front axle

$$2\Delta N_r (b_1 + a_1) - \Delta N_O a_1 - m_1 \dot{u}_1 h_1 = 0$$

gives the tractor front and rear axle normal forces as

$$\Delta N_r = (\Delta N_O a_1 + m_1 \dot{u}_1 h_1) / 2 (b_1 + a_1) \quad (34)$$

$$\Delta N_f = (\Delta N_O b_1 - m_1 \dot{u}_1 h_1) / 2 (b_1 + a_1) \quad (35)$$

3.3 Lateral Load Transfer

The lateral load transfer is derived by assuming that the load transfer resulting from lateral acceleration of the semi-trailer mass is carried by the semi-trailer axle and the tractor rear axle, while the load transfer resulting from the tractor mass is carried by the tractor front axle. This assumption is based on the roll torque transfer characteristics of the fifth wheel, the weak frame of the tractor, and the forward position of the tractor CM.

Denote by ΔN_1 the lateral load transfer of the tractor, and by ΔN_2 the load transfer of the semi-trailer. Introduce \dot{v}_1 and \dot{v}_2 to denote the vertical accelerations of the tractor and semi-trailer CMs respectively. See Figure 6. Moment balance around the right wheel of the front axle on the tractor

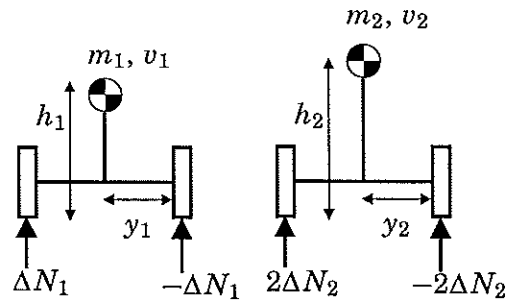


Figure 6 Lateral load transfer model.

gives

$$\Delta N_1 2y_1 = m_1 \dot{v}_1 h_1$$

and moment balance around the right wheel on the tractor rear axle and the right wheel on the semi-trailer axle gives

$$2\Delta N_2 2y_2 = m_2 \dot{v}_2 h_2$$

Then the lateral load transfer is expressed as

$$\Delta N_1 = \frac{m_1 \dot{v}_1 h_1}{2y_1} \quad (36)$$

$$\Delta N_2 = \frac{m_2 \dot{v}_2 h_2}{4y_1} \quad (37)$$

3.4 Normal Forces

Now the static load distribution together with the longitudinal and lateral load transfer gives the resulting normal forces for each individual wheel. Combining Equations (28)–(37) gives

$$\begin{aligned} N_1 &= N_f + \Delta N_f + \Delta N_1 \\ N_2 &= N_f + \Delta N_f - \Delta N_1 \\ N_3 &= N_r + \Delta N_r + \Delta N_2 \\ N_4 &= N_r + \Delta N_r - \Delta N_2 \\ N_5 &= N_t + \Delta N_t + \Delta N_2 \\ N_6 &= N_t + \Delta N_t - \Delta N_2 \end{aligned} \quad (38)$$

4. Wheel Forces and Dynamics

The wheels can modeled as rotating masses with driving or braking torques, and road contact forces determined by a tire model. The tire model gives road contact forces as a function of relative velocity of the tire and the road, and the tire slip direction.

The wheel torque T_i constitutes the system input

$$J_i \dot{\omega}_i = T_i - r_{e,i} F_i(SR, \alpha) \quad (39)$$

with $i \in \{1, 2, 3, 4, 5, 6\}$, where $F_i(SR, \alpha)$ is the tire road contact force given by the tire model. The slip ratio SR and the slip angle α are defined by Equation (40) and Figure 8 below.

5. Tire Model

The tires are modeled with the *Slip Circle Model* [SPP96], which is closely related to friction ellipse models. With this model it is possible to obtain good estimates of combined cornering and braking forces from measurement data of pure cornering and pure braking only, as in Figure 7. The motivation behind this approach is that measured tire characteristics often are available only for pure braking and cornering, while characteristics for combined braking and cornering are necessary in handling simulations.

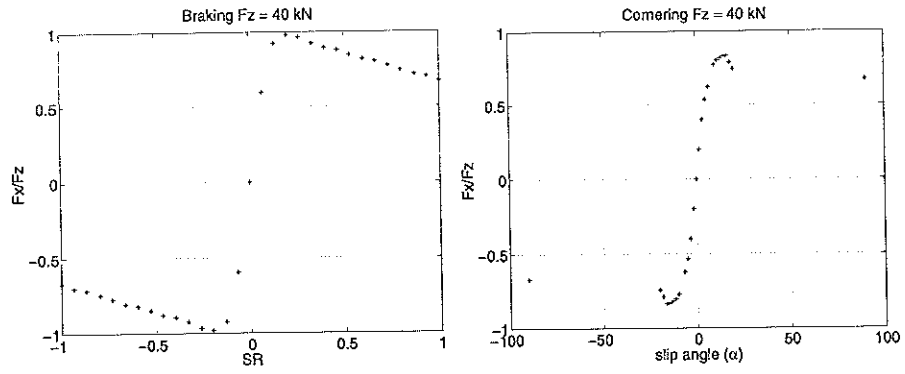


Figure 7 Measured tire characteristics for pure braking and cornering. The last data point in the cornering data is taken from pure braking with locked tire (when the tire acts as solid block of rubber).

Inputs to the model are the slip angle α and the *slip ratio*

$$(SR) = \frac{\omega R - v \cos \alpha}{\max(|v \cos \alpha|, |\omega R|)} \quad (40)$$

where R is the wheel radius, ω the rotational velocity of the wheel, and v the translational velocity of the road-tire contact point, see Figure 8.

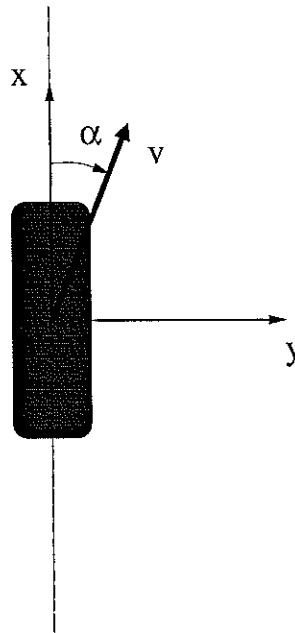


Figure 8 Tire.

A dimensionless total slip vector with magnitude s and orientation β is introduced as

$$s = \sqrt{(SR)^2 + (\sin \alpha)^2}$$

and

$$\tan \beta = -\sin \alpha / (SR)$$

The tire contact force is assumed to have the same orientation as the total slip vector, i.e.

$$\tan \beta = F_y / F_x$$

Thus $\beta = 0^\circ$ corresponds to straight line driving, $\beta = 90^\circ$ to free-rolling cornering to the right, $\beta = 180^\circ$ to pure braking, and $\beta = 270^\circ$ to free-rolling cornering to the left.

A model for combined cornering and braking is obtained by assuming a cosinusoidal fit

$$F = a_0(s) + a_1(s) \cos(2\beta)$$

where

$$a_0(s) = 0.5(F_{x,0}(s) + F_{y,0}(s))$$

$$a_1(s) = 0.5(F_{x,0}(s) - F_{y,0}(s))$$

$F_{x,0}(s)$ and $F_{y,0}(s)$ are the friction force obtained from a model of pure braking (driving) or cornering respectively.

The model predicted tire forces corresponding to the measured data in Figure 7 is shown in Figure 9. Figure 10 shows the model predicted

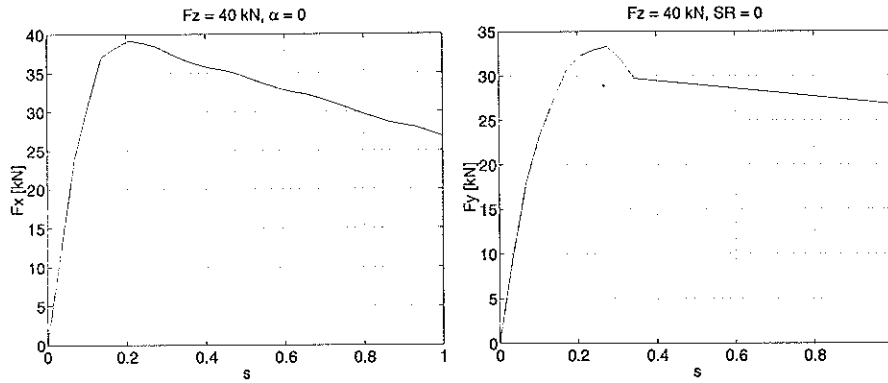


Figure 9 Model predicted forces for pure braking and cornering.

contact forces for different slip vector magnitudes and orientations. In Figure 11 the slip circle model is validated against measurements of combined braking and cornering contact forces. In Figure 12 it is shown how the tire contact-force vector can be changed by varying SR (braking/driving) or α (steering). In this plot the slip ratio is restricted to $|SR| < 0.2$, which corresponds to the working region with ABS functionality on the wheels. With arbitrary SR and α it is possible to position the force vector anywhere inside the ellipse.

6. Brake Model

The brakes are modelled as air disc brakes to be integrated with an Electrical Braking System (EBS), see [Buc98].

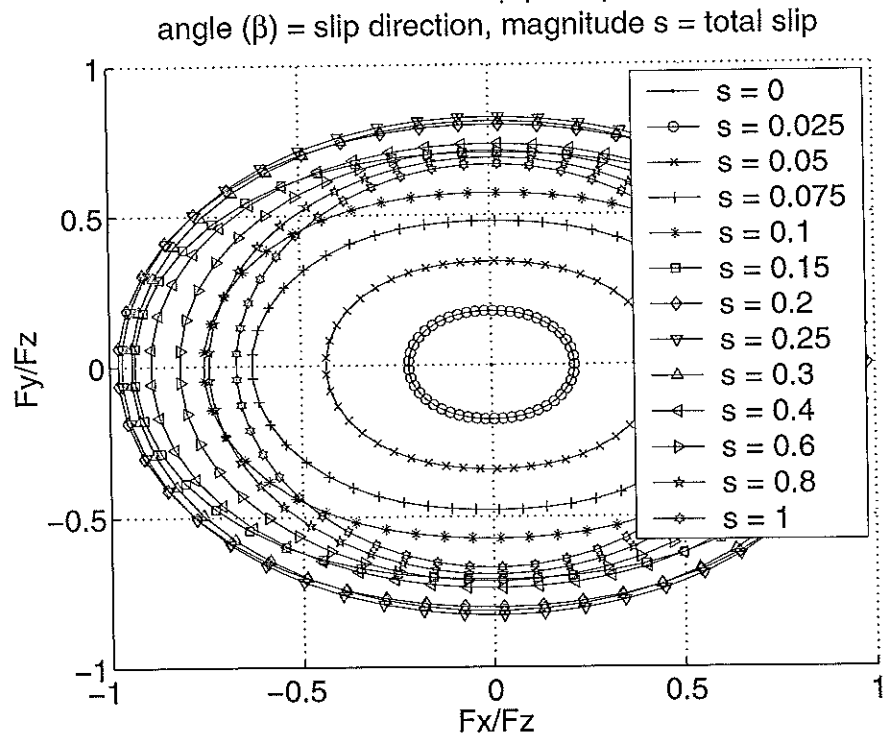


Figure 10 Polar plot of tire contact forces as a function of total slip magnitude and orientation.

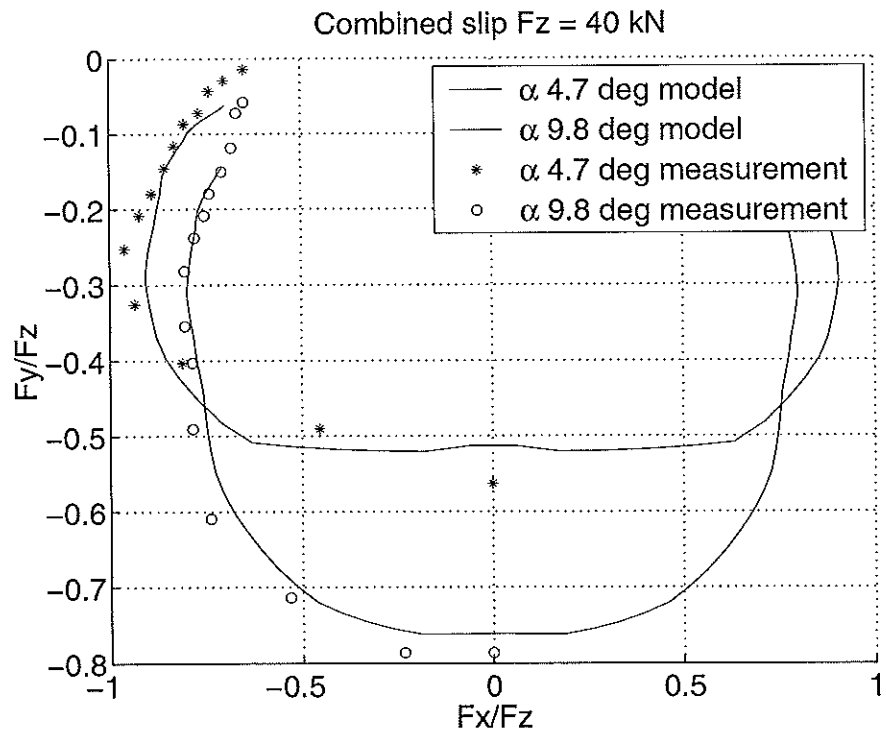


Figure 11 Validation of model predictions of tire contact forces in combined braking and cornering.

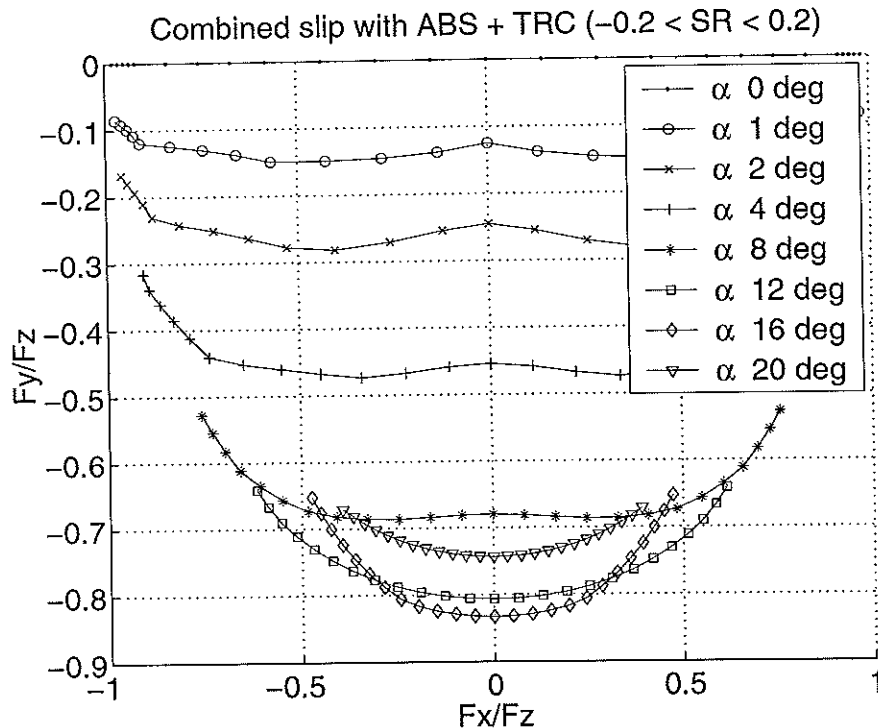


Figure 12 Combined braking and cornering for $-0.2 \leq SR \leq 0.2$ and $-20^\circ \leq \alpha \leq 20^\circ$.

The basic outline of the disc brake is a C-clamp with friction pads on both jaws. A wheel mounted rotor passes between the jaws. At brake actuation a modulation valve lets air with a base pressure p_0 flow in to a chamber to build up a pressure p , proportional to the valve control signal u . A diaphragm with area a transmits a force $N = ap$ to the brake pads. With a simple Coulomb friction model the friction surfaces on the brake pads then generates a braking force $F = -\mu N \operatorname{sgn}(\omega)$ on the rotor, where μ is the coefficient of friction for the specific brake lining material. The resulting braking torque on the wheel is $\mathcal{T} = Fr_e$, where r_e is the effective radius of the disc rotor. Assuming a linear first order model of the pressure dynamics $p = p_0/(sT + 1)u$, the resulting brake model is

$$\mathcal{T} = -\frac{K}{sT + 1}u \operatorname{sgn}(\omega) \quad (41)$$

with $K = \mu ar_e p_0$. Typical values are $K = 9 \text{ kNm}$, and $T = 0.6 \text{ s}$.

7. Linear Semi-trailer Vehicle Model

The nonlinear model of the semi-trailer vehicle may adequately describe the vehicle in a wide range of operating conditions. However, a linear model may be sufficient for small deviations from a certain stationary operating point. A linear model is also much easier to exploit for control synthesis. Therefore this section is devoted to the derivation of a linear state-space model of the vehicle.

7.1 Linearized Equations of Motion

In this section a linear model for the vehicle dynamics of motion is derived. Assume a small articulation angle ψ , such that the coordinate transformation matrix in (9) can be approximated by the identity matrix, $R \approx I$. Then (11) translates to

$$\begin{aligned}
m_1 (\dot{U}_1 - r_1^2 x_1' - r_1 V_1) &= \bar{X}_1 + X_p \\
m_1 (\dot{V}_1 + \dot{r}_1 x_1 + r_1 U_1) &= \bar{Y}_1 + Y_p \\
I_1 \dot{r}_1 + m_1 x_1 (\dot{V}_1 + U_1 r_1) &= \bar{Z}_1 \\
m_2 (\dot{U}_2 + r_2^2 x_2 - r_2 V_2) &= \bar{X}_2 - X_p \\
m_2 (\dot{V}_2 - \dot{r}_2 x_2 + r_2 U_2) &= \bar{Y}_2 - Y_p \\
I_2 \dot{r}_2 - m_2 x_2 (\dot{V}_2 + U_2 r_2) &= \bar{Z}_2
\end{aligned} \tag{42}$$

The fifth wheel reaction forces X_p and Y_p may now easily be eliminated as

$$\begin{aligned}
m_1 (\dot{U}_1 - r_1^2 x_1 - r_1 V_1) + m_2 (\dot{U}_2 + r_2^2 x_2 - r_2 V_2) &= \bar{X}_1 + \bar{X}_2 \\
m_1 (\dot{V}_1 + \dot{r}_1 x_1 + r_1 U_1) + m_2 (\dot{V}_2 - \dot{r}_2 x_2 + r_2 U_2) &= \bar{Y}_1 + \bar{Y}_2 \\
I_1 \dot{r}_1 + m_1 x_1 (\dot{V}_1 + U_1 r_1) &= \bar{Z}_1 \\
I_2 \dot{r}_2 - m_2 x_2 (\dot{V}_2 + U_2 r_2) &= \bar{Z}_2
\end{aligned} \tag{43}$$

With the small articulation angle assumption the velocity relation (12) simplifies to

$$\begin{aligned}
U_2 &= U_1 \\
V_2 &= V_1
\end{aligned} \tag{44}$$

The acceleration relation (21) together with (14) yields

$$\begin{aligned}
\dot{U}_1 - V_1 r_1 &= \dot{U}_2 - V_1 r_2 \\
\dot{V}_1 + U_1 r_1 &= \dot{V}_2 + U_1 r_2
\end{aligned} \tag{45}$$

Now combining (44) and (45) with (43) gives

$$\begin{aligned}
(m_1 + m_2) (\dot{U} - V r_1) - m_1 x_1 r_1^2 + m_2 x_2 r_2^2 &= \bar{X}_1 + \bar{X}_2 \\
(m_1 + m_2) (\dot{V} + U r_1) + m_1 x_1 \dot{r}_1 - m_2 x_2 \dot{r}_2 &= \bar{Y}_1 + \bar{Y}_2 \\
I_1 \dot{r}_1 + m_1 x_1 (\dot{V} + U r_1) &= \bar{Z}_1 \\
I_2 \dot{r}_2 - m_2 x_2 (\dot{V} + U r_1) &= \bar{Z}_2
\end{aligned} \tag{46}$$

Regard the stationary operating point in a steady state turn with free rolling wheels

$$\begin{aligned}
U &= U_0 & V &= V_0 & r_1 &= r_2 = r_0 \\
\bar{X}_1 &= 0 & \bar{Y}_1 &= \bar{Y}_1^0 & \bar{Z}_1 &= \bar{Z}_1^0 \\
\bar{X}_2 &= 0 & \bar{Y}_2 &= \bar{Y}_2^0 & \bar{Z}_2 &= \bar{Z}_2^0
\end{aligned} \tag{47}$$

At this operating point (46) reduces to

$$\begin{aligned}
-(m_1 + m_2) V_0 r_0 - m_1 x_1 r_0^2 + m_2 x_2 r_0^2 &= 0 \\
(m_1 + m_2) U_0 r_0 &= \bar{Y}_1^0 + \bar{Y}_2^0 \\
m_1 x_1 U_0 r_0 &= \bar{Z}_1^0 \\
-m_2 x_2 U_0 r_0 &= \bar{Z}_2^0
\end{aligned} \tag{48}$$

For small deviations around the operating point the state and input variables may be partitioned as

$$\begin{aligned}
U &= U_0 + \delta U & \dot{U} &= \delta \dot{U} \\
V &= V_0 + \delta V & \dot{V} &= \delta \dot{V} \\
r_1 &= r_0 + \delta r_1 & \dot{r}_1 &= \delta \dot{r}_1 \\
r_2 &= r_0 + \delta r_2 & \dot{r}_2 &= \delta \dot{r}_2 \\
\bar{X}_1 &= \delta \bar{X}_1 & \bar{X}_2 &= \delta \bar{X}_2 \\
\bar{Y}_1 &= \bar{Y}_1^0 + \delta \bar{Y}_1 & \bar{Y}_2 &= \bar{Y}_2^0 + \delta \bar{Y}_2 \\
\bar{Z}_1 &= \bar{Z}_1^0 + \delta \bar{Z}_1 & \bar{Z}_2 &= \bar{Z}_2^0 + \delta \bar{Z}_2
\end{aligned} \tag{49}$$

Inserting (49) in (46), subtracting the corresponding steady state equations from (48), and removing second order terms results in the linear dynamics

$$\begin{aligned}
(m_1 + m_2) (\delta \dot{U} - r_0 \delta V - V_0 \delta r_1) - 2m_1 x_1 \delta r_1 + 2m_2 x_2 \delta r_2 &= \delta \bar{X}_1 + \delta \bar{X}_2 \\
(m_1 + m_2) (\delta \dot{V} + r_0 \delta U + U_0 \delta r_1) + m_1 x_1 \delta \dot{r}_1 - m_2 x_2 \delta \dot{r}_2 &= \delta \bar{Y}_1 + \delta \bar{Y}_2 \\
I_1 \delta \dot{r}_1 + m_1 x_1 (\delta \dot{V} + U_0 \delta r_1 + \delta U r_0) &= \delta \bar{Z}_1 \\
I_2 \delta \dot{r}_2 + m_2 x_2 (\delta \dot{V} + U_0 \delta r_1 + \delta U r_0) &= \delta \bar{Z}_2
\end{aligned} \tag{50}$$

7.2 Linear Tire Model

Linear expressions for the tire-road contact forces may be used for small slip angles α and small slip ratios SR , as indicated by Figure 7. The slopes of the respective slip curves in the initial linear regions are denoted *braking stiffness*, C_{SR} , and *cornering stiffness*, C_α .

Regard wheel i , with steering angle s_i , lateral velocity $V_i = V_i^0 + \delta V_i$, longitudinal velocity $U_i = U_i^0 + \delta U_i$, angular velocity $\omega_i = \omega_i^0 + \delta \omega_i$, radius R , slip ratio SR_i , and normal force N_i . The longitudinal contact force for small slip ratios is

$$\begin{aligned}
X_i &= C_{SR} N_i SR_i = C_{SR} N_i \frac{U_i - R \omega_i}{U_i} = C_{SR} N_i \frac{U_i^0 + \delta U_i - R(\omega_i^0 + \delta \omega_i)}{U_i^0 + \delta U_i} \approx \\
&C_{SR} N_i \frac{U_i^0 - R \omega_i^0}{U_i^0} + C_{SR} N_i \frac{\delta U_i - R \delta \omega_i}{U_i^0} = X_i^0 + \delta X_i \tag{51}
\end{aligned}$$

and the lateral contact force for small slip angles is

$$Y_i = C_\alpha N_i (s_i - V_i/U_i) = C_\alpha N_i \left(s_i^0 + \delta s_i - \frac{V_i^0 + \delta V_i}{U_i^0 + \delta U_i} \right) \approx$$

$$C_\alpha N_i (s_i^0 - V_i^0/U_i^0) + C_\alpha N_i (\delta s_i - \delta V_i/U_i^0) = Y_i^0 + \delta Y_i \quad (52)$$

The wheel velocities are expressed by

$$\begin{aligned} U_1 &= U + y_f r_1 & V_1 &= V + a_1 r_1 \\ U_2 &= U - y_f r_1 & V_2 &= V + a_1 r_1 \\ U_3 &= U + y_r r_1 & V_3 &= V - b_1 r_1 \\ U_4 &= U - y_r r_1 & V_4 &= V - b_1 r_1 \\ U_5 &= U + y_t r_2 & V_5 &= V - b_2 r_2 \\ U_6 &= U - y_t r_2 & V_6 &= V - b_2 r_2 \end{aligned} \quad (53)$$

Inserted into (51) using (49) and identifying δX_i this gives

$$\begin{aligned} \delta X_1 &= \frac{C_{SR} N_1}{U_0} (\delta U + y_f \delta r_1 - R \delta \omega_1) & \delta X_2 &= \frac{C_{SR} N_2}{U_0} (\delta U - y_f \delta r_1 - R \delta \omega_2) \\ \delta X_3 &= \frac{C_{SR} N_3}{U_0} (\delta U + y_r \delta r_1 - R \delta \omega_3) & \delta X_4 &= \frac{C_{SR} N_4}{U_0} (\delta U - y_r \delta r_1 - R \delta \omega_4) \\ \delta X_5 &= \frac{C_{SR} N_5}{U_0} (\delta U + y_t \delta r_2 - R \delta \omega_5) & \delta X_6 &= \frac{C_{SR} N_6}{U_0} (\delta U - y_t \delta r_2 - R \delta \omega_6) \end{aligned} \quad (54)$$

It is assumed above that $1/(U_0 \pm y_{\{f,r,t\}} r_0) \approx 1/U_0$. Accordingly

$$\begin{aligned} \delta Y_1 &= \frac{C_\alpha N_1}{U_0} (U_0 \delta s_1 - \delta V + a_1 \delta r_1) & \delta Y_2 &= \frac{C_\alpha N_2}{U_0} (U_0 \delta s_2 - \delta V + a_1 \delta r_1) \\ \delta Y_3 &= \frac{C_\alpha N_3}{U_0} (U_0 \delta s_3 - \delta V - b_1 \delta r_1) & \delta Y_4 &= \frac{C_\alpha N_4}{U_0} (U_0 \delta s_4 - \delta V - b_1 \delta r_1) \\ \delta Y_5 &= \frac{C_\alpha N_5}{U_0} (U_0 \delta s_5 - \delta V - b_2 \delta r_2) & \delta Y_6 &= \frac{C_\alpha N_6}{U_0} (U_0 \delta s_6 - \delta V - b_2 \delta r_2) \end{aligned} \quad (55)$$

7.3 Complete Linear Vehicle Model

Combining (54), (55) and (10) with (50) gives a complete set of linear equations for the vehicle, with wheel steering angles δs_i and wheel velocities $\delta \omega_i$ as inputs. Introduce the state vector

$$\xi = (\delta U, \delta V, \delta r_1, \delta r_2)^T \quad (56)$$

and the input vector

$$u = (\delta \omega_1, \dots, \delta \omega_6, \delta s_1, \dots, \delta s_6)^T \quad (57)$$

Then the vehicle dynamics in a neighbourhood of the stationary operating point (47) is described by

$$E \frac{d\xi}{dt} = A\xi + Bu \quad (58)$$

with

$$E = \begin{pmatrix} m & 0 & 0 & 0 \\ 0 & m & m_1 x_1 & -m_2 x_2 \\ 0 & m_1 x_1 & I_1 & 0 \\ 0 & m_2 x_2 & 0 & I_2 \end{pmatrix}$$

which is non-singular for $mI_1I_2 - m_1^2x_1^2I_2 + m_2^2x_2^2I_1 \neq 0$. The system matrix $A = (a_{ij})$, $i = 1 \dots 4$, $j = 1 \dots 4$ has the elements

$$\begin{aligned}
a_{11} &= \frac{C_{SR}}{U_0}(N_1 + N_2 + N_3 + N_4 + N_5 + N_6) = \frac{C_{SR}}{U_0}mg \\
a_{12} &= mr_0 \\
a_{13} &= mV_0 + 2m_1x_1 + \frac{C_{SR}}{U_0}(y_f(N_1 - N_2) + y_r(N_3 - N_4)) \\
&= mV_0 + 2m_1x_1 + \frac{C_{SR}}{U_0}(2y_f\Delta N_1 + 2y_r\Delta N_2) \\
a_{14} &= -2m_2x_2 + \frac{C_{SR}}{U_0}y_t(N_5 - N_6) = -2m_2x_2 + \frac{C_{SR}}{U_0}2y_t\Delta N_2 \\
a_{21} &= -mr_0 \\
a_{22} &= -\frac{C_\alpha}{U_0}(N_1 + N_2 + N_3 + N_4 + N_5 + N_6) = -\frac{C_\alpha}{U_0}mg \\
a_{23} &= mV_0 + \frac{C_\alpha}{U_0}(a_1(N_1 + N_2) - b_1(N_3 + N_4)) \\
&= mV_0 + \frac{C_\alpha}{U_0}(2a_1(N_f + \Delta N_f) - 2b_1(N_r + \Delta N_r)) \\
a_{24} &= -\frac{C_\alpha}{U_0}b_2(N_5 + N_6) = -\frac{C_\alpha}{U_0}2b_2(N_t + \Delta N_t) \\
a_{31} &= -m_1x_1r_0 + \frac{C_{SR}}{U_0}(y_f(N_1 - N_2) + y_r(N_3 - N_4)) \\
&= -m_1x_1r_0 + \frac{C_{SR}}{U_0}(2y_f\Delta N_1 + 2y_r\Delta N_2) \\
a_{32} &= \frac{C_\alpha}{U_0}(-a_1(N_1 + N_2) + b_1(N_3 + N_4)) \\
&= \frac{C_\alpha}{U_0}(-2a_1(N_f + \Delta N_f) + 2b_1(N_r + \Delta N_r)) \\
a_{33} &= -m_1x_1U_0 + \frac{C_{SR}}{U_0}(y_f^2(N_1 + N_2) + y_r^2(N_3 + N_4)) + \\
&\quad \frac{C_\alpha}{U_0}(a_1^2(N_1 + N_2) + b_1^2(N_3 + N_4)) \\
&= -m_1x_1U_0 + \frac{C_{SR}}{U_0}(2y_f^2(N_f + \Delta N_f) + 2y_r^2(N_r + \Delta N_r)) + \\
&\quad \frac{C_\alpha}{U_0}(2a_1^2(N_f + \Delta N_f) + 2b_1^2(N_r + \Delta N_r)) \\
a_{34} &= 0 \\
a_{41} &= -m_2x_2r_0 \frac{C_{SR}}{U_0}y_t(N_5 - N_6) = -m_2x_2r_0 \frac{C_{SR}}{U_0}2y_t\Delta N_2 \\
a_{42} &= \frac{C_\alpha}{U_0}b_2(N_5 + N_6) = \frac{C_\alpha}{U_0}2b_2(N_t + \Delta N_t) \\
a_{43} &= -m_2x_2U_0 \\
a_{44} &= \frac{C_{SR}}{U_0}y_t^2(N_5 + N_6) + \frac{C_\alpha}{U_0}b_2^2(N_5 + N_6) \\
&= \frac{C_{SR}}{U_0}2y_t^2(N_t + \Delta N_t) + \frac{C_\alpha}{U_0}2b_2^2(N_t + \Delta N_t)
\end{aligned} \tag{59}$$

The input gain matrix is

$$B^T = \begin{pmatrix} -C_{SR}RN_1/U_0 & 0 & -C_{SR}Ry_fN_1/U_0 & 0 \\ -C_{SR}RN_2/U_0 & 0 & C_{SR}Ry_fN_2/U_0 & 0 \\ -C_{SR}RN_3/U_0 & 0 & -C_{SR}Ry_rN_3/U_0 & 0 \\ -C_{SR}RN_4/U_0 & 0 & C_{SR}Ry_rN_4/U_0 & 0 \\ -C_{SR}RN_5/U_0 & 0 & 0 & -C_{SR}Ry_tN_5/U_0 \\ -C_{SR}RN_6/U_0 & 0 & 0 & C_{SR}Ry_tN_6/U_0 \\ 0 & C_\alpha N_1 & C_\alpha a_1 N_1 & 0 \\ 0 & C_\alpha N_2 & C_\alpha a_1 N_2 & 0 \\ 0 & C_\alpha N_3 & -C_\alpha b_1 N_3 & 0 \\ 0 & C_\alpha N_4 & -C_\alpha b_1 N_4 & 0 \\ 0 & C_\alpha N_5 & 0 & -C_\alpha b_2 N_5 \\ 0 & C_\alpha N_6 & 0 & -C_\alpha b_2 N_6 \end{pmatrix}$$

Partitioning of normal forces according to (38) illustrates the effect of load transfer on A and B . The load transfer may be regarded as parametric uncertainties. This is explicitly shown in (59), where certain terms only appear at load transfer.

Note that the choice of state variables in (58) is different from that of (25). A simple linear state transformation may be applied on the linear model to achieve the same state description.

8. Simulink Model

The nonlinear semi-trailer vehicle model with wheel and brake dynamics, and slip-circle tire-road contact model is implemented in Matlab/Simulink. Listings of the S-function, and some essential m-files are found in Appendix B.

8.1 Simulation Example

In this section a simulation scenario for a specific vehicle configuration is presented. The vehicle geometry and mass distribution is listed in Tables 1 – 3. The tire characteristics are those of Figure 7. The simulation

α_1 [m]	b_1 [m]	x_1 [m]	y_f [m]	y_r [m]	b_2 [m]	x_2 [m]	y_t [m]
2.8	0.7	1.8	1.0	1.0	14	7.0	1.0

Table 1 Vehicle geometric configuration

scenario is described in Table 4 below. A trace of the simulation is shown in Figure 13. A close-up on the vehicle at $t \approx 35$ s is shown in Figure 14. More plots of the simulation are presented in Appendix A.

$m_1[kg]$	$m_2[kg]$	$I_1 [kgm^2]$	$I_2 [kgm^2]$
7050	23500	$5650 + m_1 x_1^2$	$390300 + m_2 x_2^2$

Table 2 Vehicle inertial configuration

$r[m]$	$m[kg]$	$I [kgm^2]$
0.4	200	$mr^2/2$

Table 3 Wheel configuration

$t [s]$	Action
5	apply half braking power on tractor left wheels
10	release brakes
15	steer left 2° with tractor rear wheels
20	straight driving
25	steer right 5° with tractor front wheels
30	steer left 5° with tractor front wheels
35	apply full braking power on all wheels

Table 4 Simulation scenario

9. Validation

To validate the nonlinear model a multi-body system (MBS) model of similar complexity has been constructed. Outputs from simulations of the two models are compared in this section. The MBS tool used is COMPAMM (COMPUter Analysis of Machines and Mechanisms) from CEIT (Centro de Estudios e Investigaciones Tecnicas de Guipuzcoa) 1999.

9.1 The Multi-body Simulation Model

In a multi body simulation model a set of rigid bodies are interconnected by joints. A body is defined by the physical properties: mass, center of gravity and inertia tensors. Points and vectors on the body can also be defined. There are several kinds of joints, for example: cylindrical, spherical and revolute. Joints can be assigned spring and damper characteristics. The dynamic simulation is driven by forces acting on the multi body system. Each body uses its local coordinate system. The relative initial placements of bodies is defined in the global coordinate system attached to the ground. The bodies are influenced by inertial forces and gravitation and the forces in the interconnecting joints.

The tractor consists of two bodies: the sprung and unsprung masses, see Figure 15. The semi-trailer also consists of two bodies: the sprung and unsprung masses, with the sprung mass connected to the unsprung mass of the tractor with a spherical joint. The sprung mass can roll relative to the unsprung mass. The contact with the road is modelled with bodies without masses interconnected by prismatic joints (a prismatic joint only

allows movement in along a straight line) and revolute joints. Thus both the unsprung mass of the truck and semi-trailer can move freely in a horizontal plane. The model is a bicycle model with three wheels: two for the truck and one for the semi-trailer. The setpoint is the front wheel steering angle and longitudinal brake slip for each wheel. The corresponding force vectors are calculated as described in Section 5 and applied to the multi body system.

9.2 Comparisions

A scenario with combined braking and cornering has been used for the validation simulations. The Simulink model uses wheel torques and wheel angles as system inputs, while the COMPAMM model uses slip ratios and wheel angles. Therefore the resulting slip ratios from the Simulink simulations have been used as inputs to the COMPAMM model. Results of the simlations are shown in Figure 16.

It is clear that the two models behave qualitatively similar, even though there are minor discrepances.

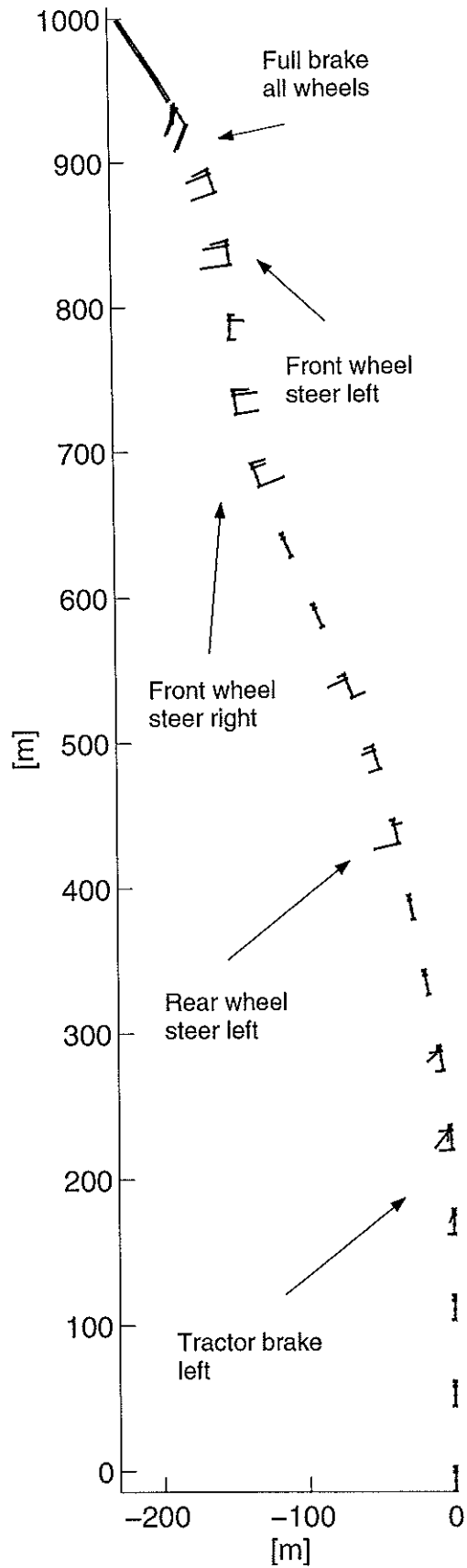


Figure 13 Trace of vehicle path, with tire-road contact force vectors.

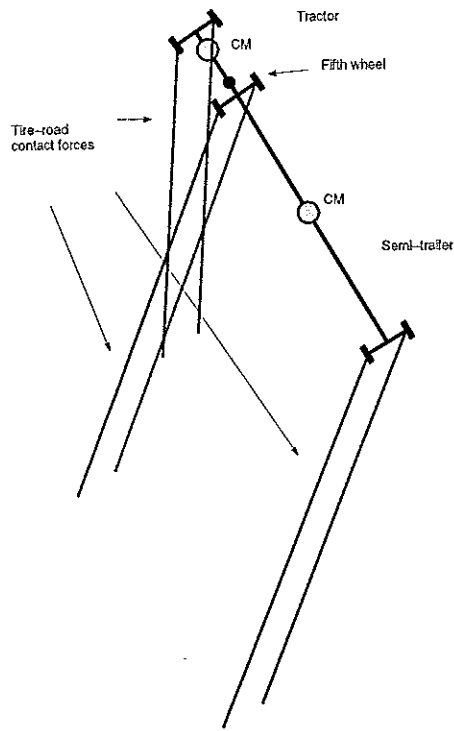


Figure 14 Snapshot of vehicle during front wheel left turn and braking.

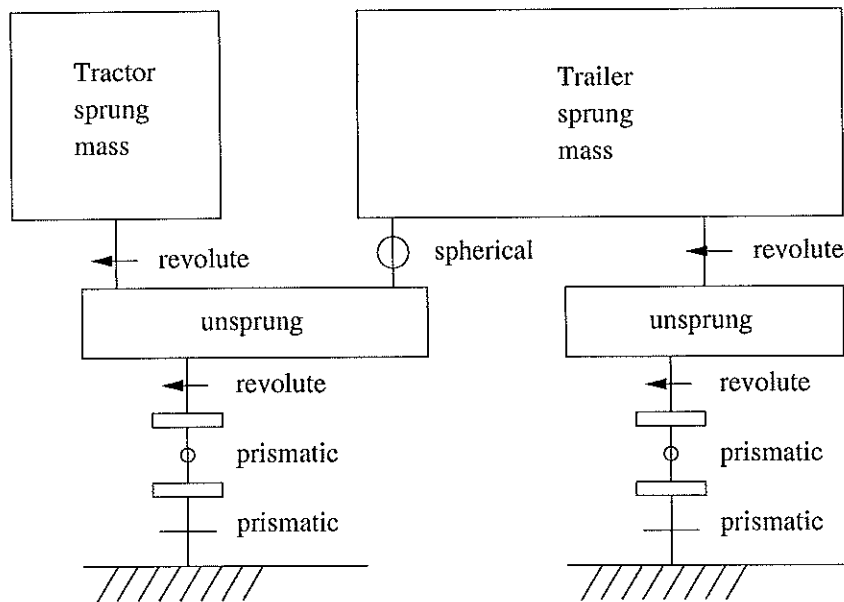


Figure 15 Multi body system model of the truck and semitrailer.

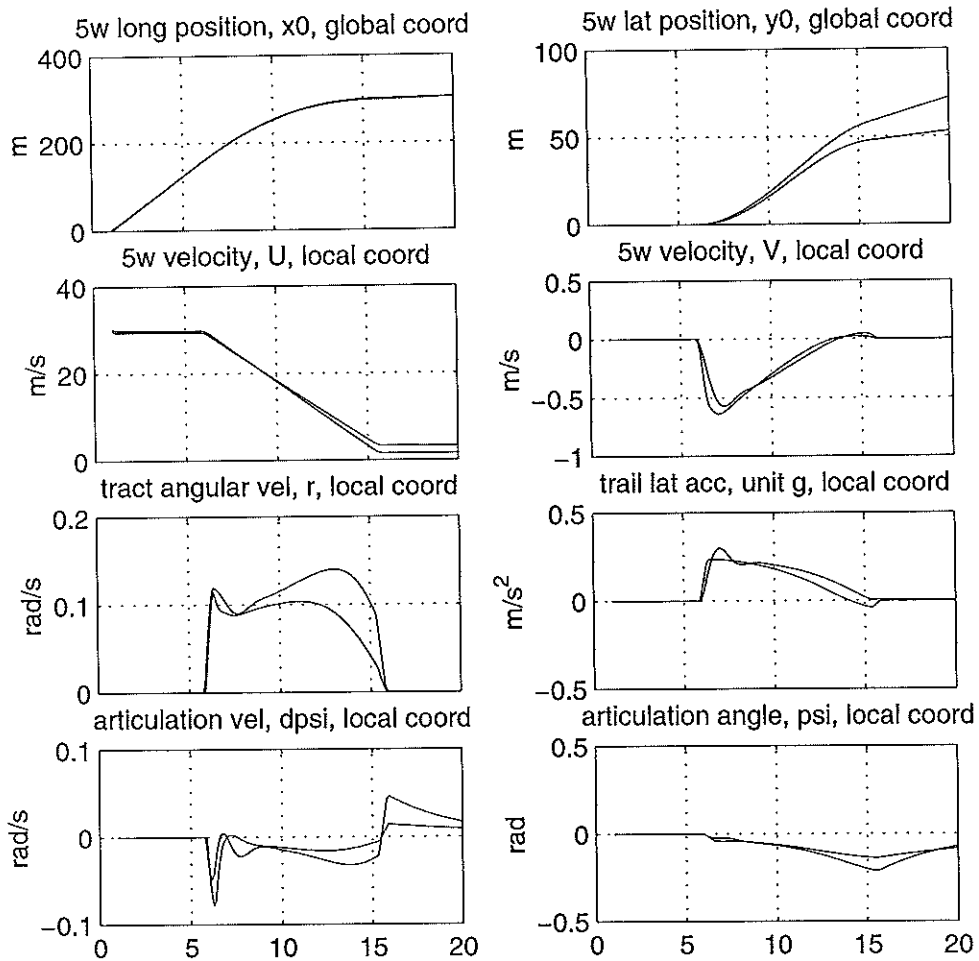


Figure 16 Comparison between Simulink and MBS simulation.

Acknowledgements

This work is part of the DICOSMOS (DIstributed COntrol of Safety critical MOTion Systems!) project, funded by NUTEK under the Complex Technical Systems program, with project nr. P11762-2, and by Volvo Technological Development (VTD). Mats Andersson (VTD) has been an initiator of the work on the semi-trailer combination vehicle, and has been a valuable source of information and ideas. Thanks to Sven Hedlund for fruitful discussions during the work on the equations of motion, and to Olof Lindgärde (VTD) for proof-reading and checking the equations.

10. References

- [Buc98] Leonard C. Buckman. *Commercial Vehicle Braking Systems: Air Brakes, ABS and Beyond*. Number SP-1405. SAE International, 1998.
- [CT00] Chieh Chen and Masayoshi Tomizuka. Lateral control of commercial heavy vehicles. *Vehicle System Dynamics*, (33):391–420, 2000.
- [Ell69] John Ronaine Ellis. *Vehicle Dynamics*. Business Books Ltd., London, 1969.
- [Ell94] J.R. Ellis. *Vehicle Handling Dynamics*. Mechanical Engineering Publications Limited, London, 1994.
- [FC93] Grant R. Fowles and George L. Cassiday. *Analytical Mechanics*. Saunders College Publishing, 5 edition, 1993.
- [Leu70] Philip M. Leucht. The directional dynamics of the commercial tractor-semitrailer vehicle during braking. Technical Report SAE Paper 700371, Society of Automotive Engineers, 1970.
- [Mit90] Manfred Mitschke. *Dynamik der Kraftfahrzeuge, Band C: Fahrverhalten*. Springer-Verlag, 2nd edition, 1990.
- [SPP96] Dietrich J. Schuring, Wolfgang Pelz, and Marion G. Pottinger. A model for combined tire cornering and braking forces. In *Investigations and Analysis in Vehicle Dynamics and Simulation*, pages 61–83. SAE International, 1996. SAE Paper 960180.

A. Simulation Example Plots

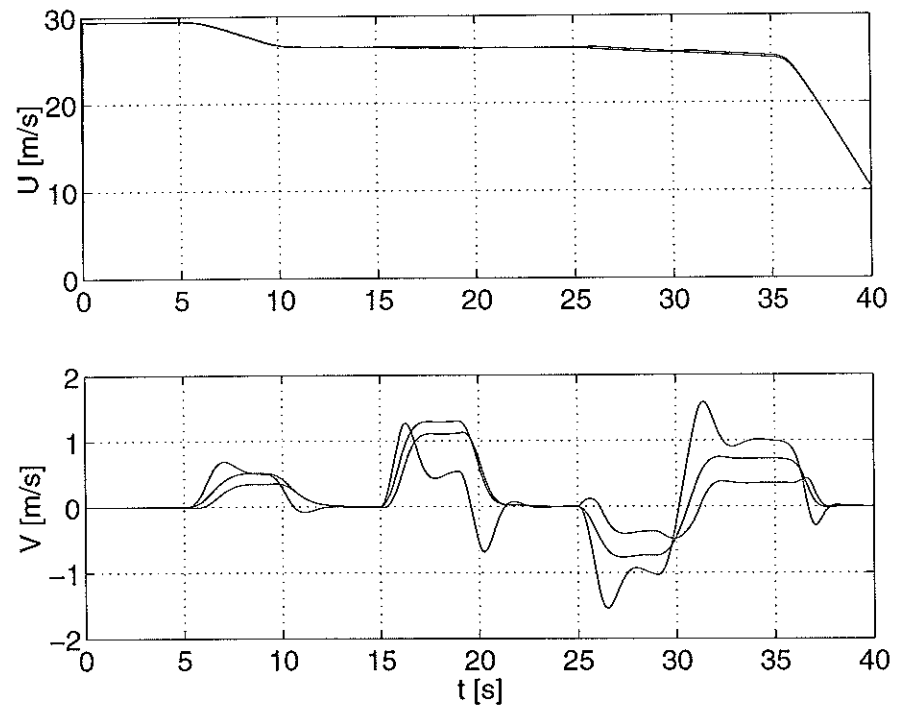


Figure 17 Vehicle (fifth wheel) longitudinal U and lateral V speed.

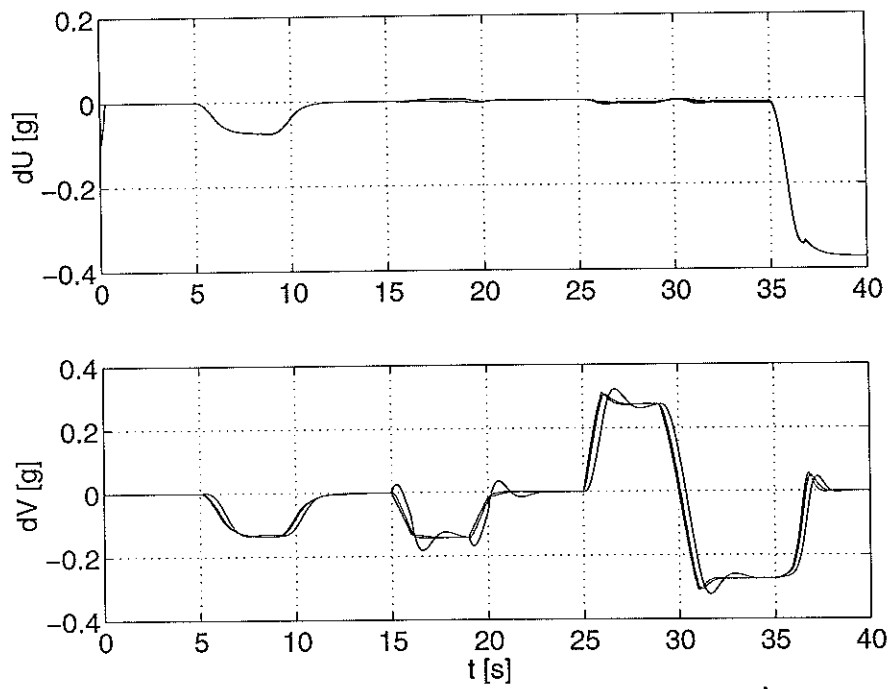


Figure 18 Longitudinal \dot{U} and lateral \dot{V} accelerations for fifth wheel, tractor CM and semi-trailer CM. A rule of thumb is that rollover may occur for lateral accelerations greater than approximately 0.4 g.

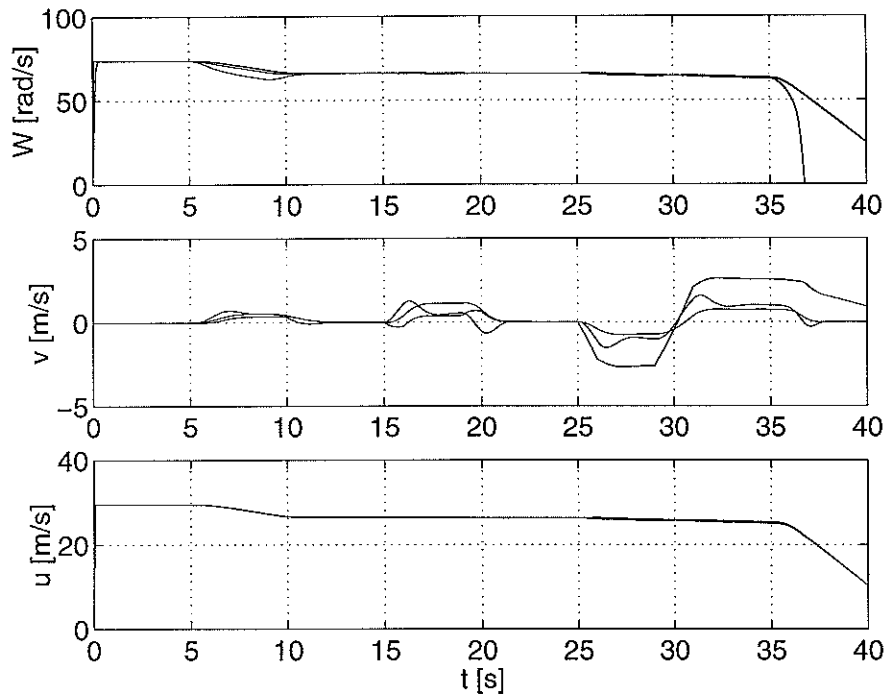


Figure 19 Wheel speeds W and vehicle longitudinal U and lateral V speed at the wheel positions. Note the front wheel lock at $t \approx 37$ s.

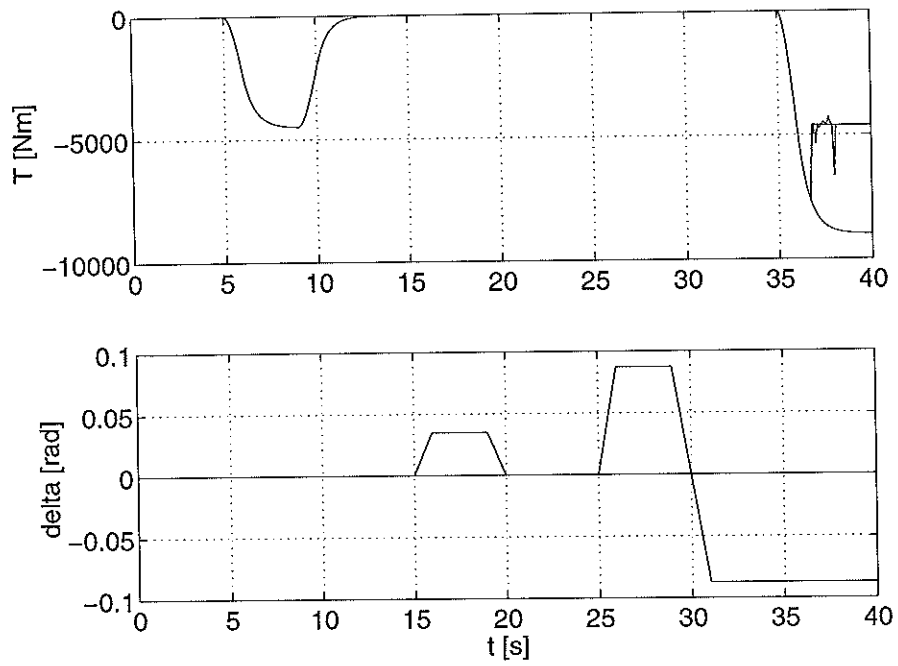


Figure 20 Braking torques T and wheel steering angles δ . Note how the braking torque drops off as the front wheels lock.

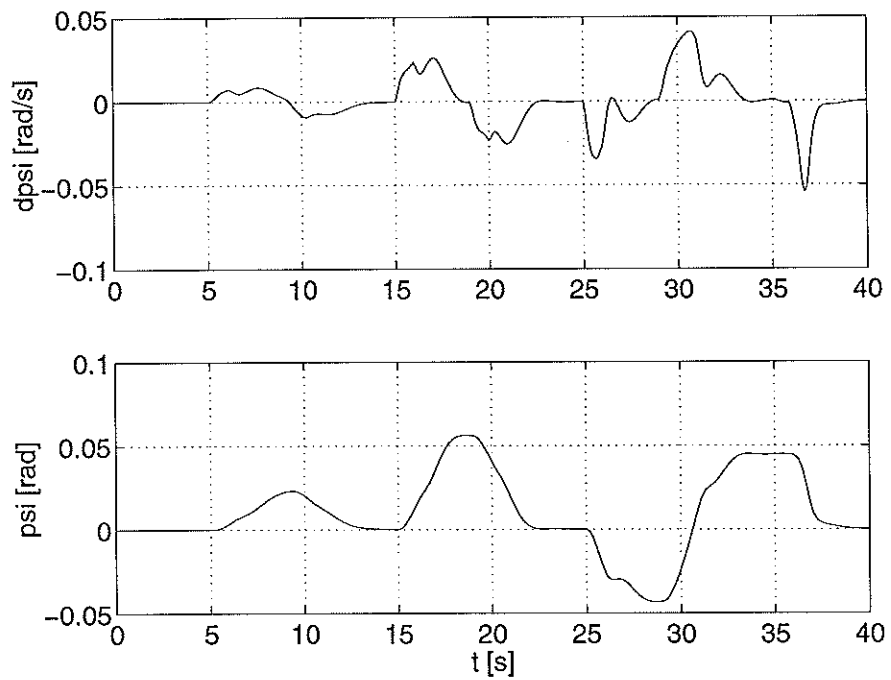


Figure 21 Articulation angle ψ , and rate of change of articulation angle $\dot{\psi}$.

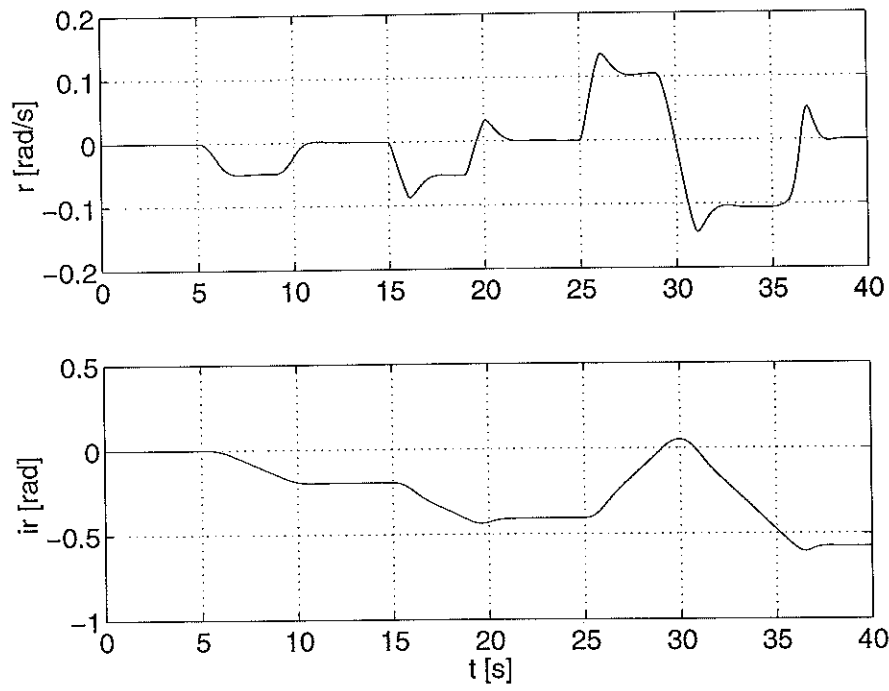


Figure 22 Tractor yaw velocity r , and orientation $\int r$.

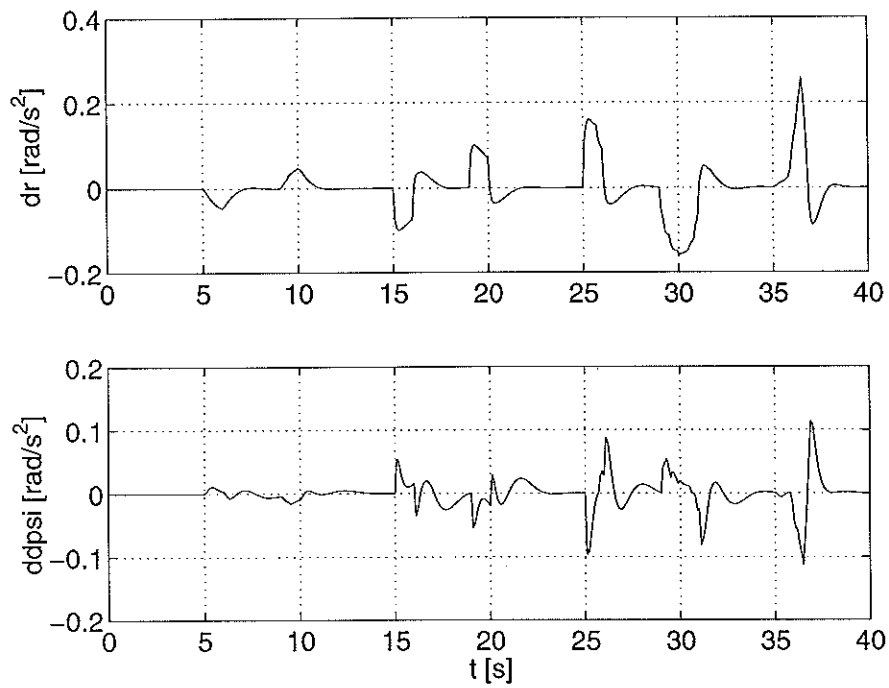


Figure 23 Tractor yaw acceleration \dot{r} , and articulation angle acceleration $\ddot{\psi}$.

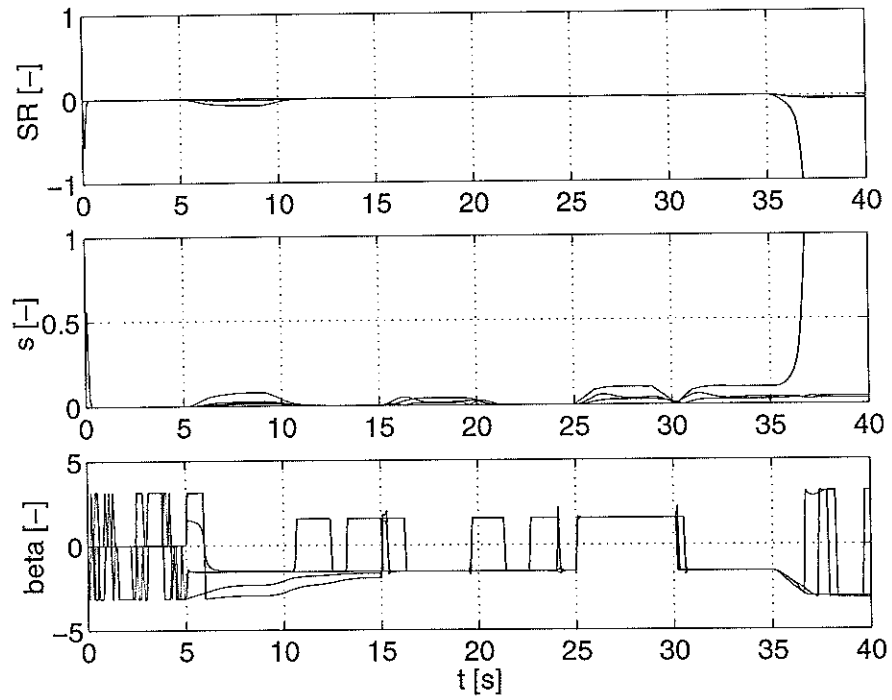


Figure 24 Tire slip ratio SR , slip vector magnitude s and slip angle orientation β . The apparent chattering of β is due to the value domain of the atan2 function in Matlab, and corresponds to rounding errors when the slip vectors are aligned parallel with the wheels. This poses no problems in the simulation, since β only is used as arguments to trigonometric functions that still give continuous output. Note the wheel slips as the front wheels lock at $t \approx 37$ s.

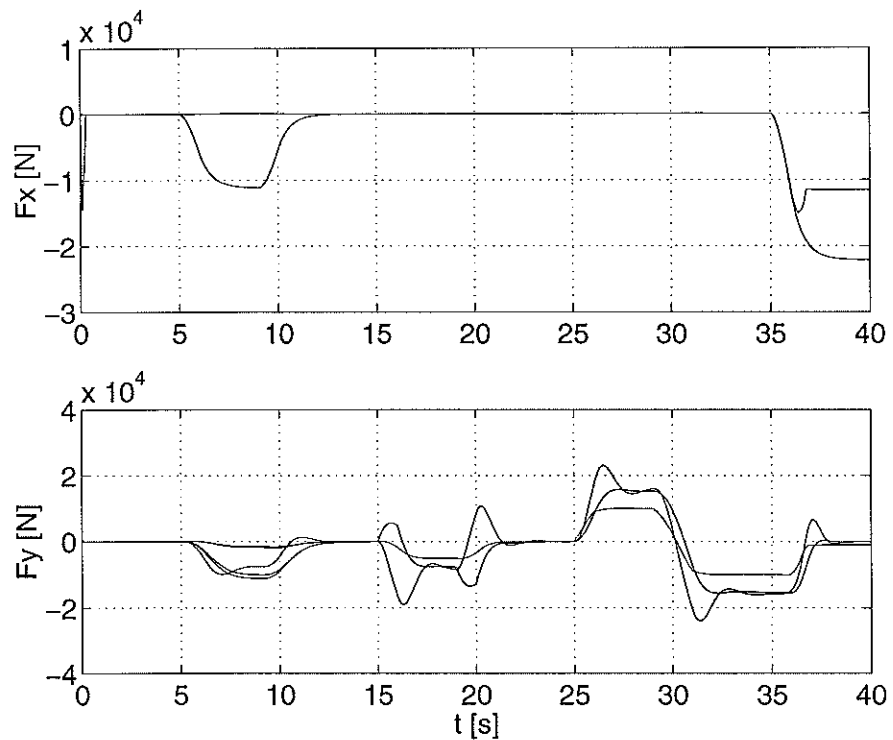


Figure 25 Generated tire forces F_x and F_y in wheel coordinates.

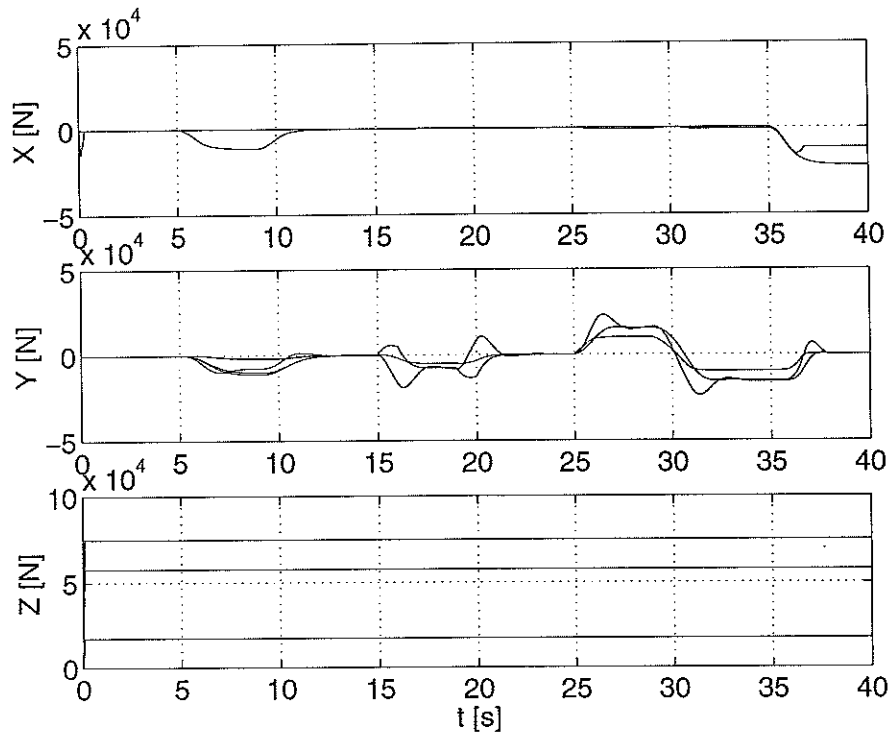


Figure 26 Tire forces X and Y in vehicle coordinates, and normal forces N .

B. Simulink Model Source

This section lists the Matlab code for some of the routines used for the simulations.

Matlab S-function

```
function [sys,x0,str,ts] = truck_sfun(t,x,u,flag,v0,vd,wd,td)
persistent data;
```

```
switch flag,
```

```
    %%%%%%%%%%%
    % Initialization %
    %%%%%%%%%%%
```

```
case 0,
    [sys,x0,str,ts,data]=mdlInitializeSizes(v0,data);
```

```
    %%%%%%%%%%%
    % Derivatives %
    %%%%%%%%%%%
```

```
case 1,
    [sys,data]=mdlDerivatives(t,x,u,vd,wd,td,data);
```

```
    %%%%%%%%%%%
    % Update %
    %%%%%%%%%%%
```

```
case 2,
    sys=mdlUpdate(t,x,u);
```

```
    %%%%%%%%%%%
    % Outputs %
    %%%%%%%%%%%
```

```
case 3,
    sys=mdlOutputs(t,x,u,vd,data);
```

```
    %%%%%%%%%%%
    % GetTimeOfNextVarHit %
    %%%%%%%%%%%
```

```
case 4,
    sys=mdlGetTimeOfNextVarHit(t,x,u);
```

```
    %%%%%%%%%%%
    % Terminate %
    %%%%%%%%%%%
```

```
case 9,
    sys=mdlTerminate(t,x,u);
```

```
    %%%%%%%%%%%
    % Unexpected flags %
    %%%%%%%%%%%
```

```
otherwise
    error(['Unhandled flag = ',num2str(flag)]);
```

```

end

%
%=====
% mdlInitializeSizes
% Return the sizes, initial conditions, and sample times for the S-function.
%=====
%
function [sys,x0,str,ts,data]=mdlInitializeSizes(v0,data)

sizes = simsizes;

data = zeros(108,1);

sizes.NumContStates = 14;
x0 = zeros(1,sizes.NumContStates);
sizes.NumDiscStates = 0;
sizes.NumOutputs = 1 +length(data);
sizes.NumInputs = 12;
sizes.DirFeedthrough = 0;
sizes.NumSampleTimes = 1; % at least one sample time is needed

sys = simsizes(sizes);
x0(1) = v0/100;

str = [];

ts = [0 0];

% end mdlInitializeSizes

%
%=====
% mdlDerivatives
% Return the derivatives for the continuous states.
%=====
%
function [sys,data]=mdlDerivatives(t,x,u,vd,wd,td,data)

% U longitudinal velocity at fifth wheel in tractor coordinates
% V lateral velocity at fifth wheel in tractor coordinates
% r yaw rate
% dpsi articulation angular velocity
% ir yaw
% psi articulation angle
% x0 fifth wheel position in global coordinates
% y0 fifth wheel position in global coordinates
% W wheel velocities
U = x(1)*100;
V = x(2);
r = x(3);

```



```

dpsi = x(4);
ir = x(5);
psi = x(6);
x0 = x(7);
y0 = x(8);
W1 = x(9)*100;
W2 = x(10)*100;
W3 = x(11)*100;
W4 = x(12)*100;
W5 = x(13)*100;
W6 = x(14)*100;

% wheel steering angles
delta1 = u(1);
delta2 = u(2);
delta3 = u(3);
delta4 = u(4);
delta5 = u(5);
delta6 = u(6);

% wheel torques (negative braking, positive driving)
b = 50;
T1 = -atan(W1*b)*u(7)*2/pi*1000;
T2 = -atan(W2*b)*u(8)*2/pi*1000;
T3 = -atan(W3*b)*u(9)*2/pi*1000;
T4 = -atan(W4*b)*u(10)*2/pi*1000;
T5 = -atan(W5*b)*u(11)*2/pi*1000;
T6 = -atan(W6*b)*u(12)*2/pi*1000;

cospsi = cos(psi);
sinpsi = sin(psi);

cosir = cos(ir);
sinir = sin(ir);

% longitudinal velocities at wheel positions in vehicle coordinates
U1 = (U+vd.yf*r);
U2 = (U-vd.yf*r);
U3 = (U+vd.yr*r);
U4 = (U-vd.yr*r);
U5 = (U*cospsi + V*sinpsi + vd.yt*(r+dpsi));
U6 = (U*cospsi + V*sinpsi - vd.yt*(r+dpsi));

% lateral velocities at wheel positions in vehicle coordinates
V1 = V+vd.a1*r;
V2 = V+vd.a1*r;
V3 = V-vd.b1*r;
V4 = V-vd.b1*r;
V5 = -U*sinpsi + V*cospsi - vd.b2*(r+dpsi);
V6 = -U*sinpsi + V*cospsi - vd.b2*(r+dpsi);

% longitudinal velocities at wheel positions in wheel coordinates

```

```

u1 = cos(delta1)*U1 + sin(delta1)*V1;
u2 = cos(delta2)*U2 + sin(delta2)*V2;
u3 = cos(delta3)*U3 + sin(delta3)*V3;
u4 = cos(delta4)*U4 + sin(delta4)*V4;
u5 = cos(delta5)*U5 + sin(delta5)*V5;
u6 = cos(delta6)*U6 + sin(delta6)*V6;

% lateral velocities at wheel positions in wheel coordinates
v1 = -sin(delta1)*U1 + cos(delta1)*V1;
v2 = -sin(delta2)*U2 + cos(delta2)*V2;
v3 = -sin(delta3)*U3 + cos(delta3)*V3;
v4 = -sin(delta4)*U4 + cos(delta4)*V4;
v5 = -sin(delta5)*U5 + cos(delta5)*V5;
v6 = -sin(delta6)*U6 + cos(delta1)*V6;

g = 9.8;

% normal forces
mu = 1;
Fz1 = vd.m1/4*g*mu;
Fz2 = vd.m1/4*g*mu;
Fz3 = (vd.m1+vd.m2)/4*g*mu;
Fz4 = (vd.m1+vd.m2)/4*g*mu;
Fz5 = vd.m2/4*g*mu;
Fz6 = vd.m2/4*g*mu;

% computation of tire slips and tire/road contact forces
% Fx, Fy tire/road contact forces in wheel coordinates
% SR slip ratio
% s slip vector magnitude
% slip direction
% mux, muy tire/road friction coefficients in vehicle coordinates
% function [Fx,Fy,SR,s,beta] = combinatormu(vx,vy,vw,Fxmodel,Fymodel,xdata,ydata)

[mux1,muy1,SR1,s1,beta1] = combinatormu(u1,v1, ...
    wd.r*W1, td.xmodel,td.ymodel, ...
    td.xdata,td.ydata);
Fx1 = mux1*Fz1;
Fy1 = muy1*Fz1;
X1 = cos(delta1)*Fx1 - sin(delta1)*Fy1;
Y1 = sin(delta1)*Fx1 + cos(delta1)*Fy1;

[mux2,muy2,SR2,s2,beta2] = combinatormu(u2,v2, ...
    wd.r*W2,td.xmodel, td.ymodel, ...
    td.xdata,td.ydata);
Fx2 = mux2*Fz2;
Fy2 = muy2*Fz2;
X2 = cos(delta2)*Fx2 - sin(delta2)*Fy2;
Y2 = sin(delta2)*Fx2 + cos(delta2)*Fy2;

[mux3,muy3,SR3,s3,beta3] = combinatormu(u3,v3, ...

```

```

        wd.r*W3,td.xmodel,td.ymodel, ...
        td.xdata,td.ydata);
Fx3 = mux3*Fz3;
Fy3 = muy3*Fz3;
X3 = cos(delta3)*Fx3 - sin(delta3)*Fy3;
Y3 = sin(delta3)*Fx3 + cos(delta3)*Fy3;

[mux4,muy4,SR4,s4,beta4] = combinatormu(u4,v4, ...
        wd.r*W4,td.xmodel,td.ymodel, ...
        td.xdata,td.ydata);
Fx4 = mux4*Fz4;
Fy4 = muy4*Fz4;
X4 = cos(delta4)*Fx4 - sin(delta4)*Fy4;
Y4 = sin(delta4)*Fx4 + cos(delta4)*Fy4;

[mux5,muy5,SR5,s5,beta5] = combinatormu(u5,v5, ...
        wd.r*W5,td.xmodel,td.ymodel, ...
        td.xdata,td.ydata);
Fx5 = mux5*Fz5;
Fy5 = muy5*Fz5;
X5 = cos(delta5)*Fx5 - sin(delta5)*Fy5;
Y5 = sin(delta5)*Fx5 + cos(delta5)*Fy5;

[mux6,muy6,SR6,s6,beta6] = combinatormu(u6,v6, ...
        wd.r*W6,td.xmodel,td.ymodel, ...
        td.xdata,td.ydata);
Fx6 = mux6*Fz6;
Fy6 = muy6*Fz6;
X6 = cos(delta6)*Fx6 - sin(delta6)*Fy6;
Y6 = sin(delta6)*Fx6 + cos(delta6)*Fy6;

% A*dx/dt = B
A(1,1) = vd.m1 + vd.m2;
A(1,2) = 0;
A(1,3) = vd.m2*vd.x2*sinpsi;
A(1,4) = vd.m2*vd.x2*sinpsi;
A(2,1) = 0;
A(2,2) = vd.m1 + vd.m2;
A(2,3) = vd.m1*vd.x1 - vd.m2*vd.x2*cospsi;
A(2,4) = -vd.m2*vd.x2*cospsi;
A(3,1) = 0;
A(3,2) = vd.m1*vd.x1;
A(3,3) = vd.I1;
A(3,4) = 0;
A(4,1) = -vd.m2*vd.x2*sinpsi;
A(4,2) = vd.m2*vd.x2*cospsi;
A(4,3) = vd.I2;
A(4,4) = vd.I2;

B(1) = (vd.m1+vd.m2)*V*r + vd.m1*vd.x1*r^2 - vd.m2*vd.x2*(r+dpsi)^2*cospsi ..
        + X1 + X2 + X3 + X4 + (X5+X6)*cospsi - (Y5+Y6)*sinpsi;
B(2) = -(vd.m1+vd.m2)*U*r - vd.m2*vd.x2*(r+dpsi)^2*sinpsi + Y1 + Y2 ...

```

```

    + Y3 + Y4 + (Y5+Y6)*cospsi - (X5+X6)*sinpsi;
%B(3) = vd.a1*(Y1+Y2) - vd.b1*(Y3+Y4) + vd.yf*(X1-X2) ...
%      + vd.yr*(X3-X4);
B(3) = -vd.m1*vd.x1*U*r + vd.a1*(Y1+Y2) - vd.b1*(Y3+Y4) + vd.yf*(X1-X2) ...
      + vd.yr*(X3-X4);
%B(4) = -vd.m2*vd.x2*dpsi*(U*cospsi+V*sinpsi) - vd.b2*(Y5+Y6) + vd.yt* ...
%      (X5-X6);
B(4) = vd.m2*vd.x2*r*(U*cospsi+V*sinpsi) - vd.b2*(Y5+Y6) + vd.yt* ...
      (X5-X6);

sys = [A\B'; r; dpsi ; cosir*U - sinir*V; sinir*U + cosir*V; ...
      1/wd.I*(T1-wd.r*Fx1); 1/wd.I*(T2-wd.r*Fx2); 1/wd.I* ...
      (T3-wd.r*Fx3); 1/wd.I*(T4-wd.r*Fx4); 1/wd.I*(T5-wd.r*Fx5); ...
      1/wd.I*(T6-wd.r*Fx6)];

sys(1) = sys(1)/100;
sys(9:14) = sys(9:14)/100;

dU = sys(1)*100;
dV = sys(2);
dr = sys(3);
ddpsi = sys(4);

% CG accelerations
dU0 = dU - r*V;
dV0 = dV + r*U;
dU1 = dU - r^2*vd.x1 - r*V;
dV1 = dV + dr*vd.x1 + r*U;
dU2 = (dU + V*dpsi)*cospsi + (dV - U*dpsi)*sinpsi + (r + dpsi)^2*vd.x2 ...
      - (r + dpsi)*(-U*sinpsi + V*cospsi);
dV2 = -(dU + V*dpsi)*sinpsi + (dV - U*dpsi)*cospsi - (dr + ddpsi)*vd.x2 ...
      + (r + dpsi)*(U*cospsi + V*sinpsi);

data = [U; V; r; dpsi; ir; psi; x0; y0; W1; W2; W3; W4; W5; W6;...
      Fx1; Fx2; Fx3; Fx4; Fx5; Fx6; Fy1; Fy2; Fy3; Fy4; ...
      Fy5; Fy6; SR1; SR2; SR3; SR4; SR5; SR6; s1; s2; s3; s4; s5; ...
      s6; beta1; beta2; beta3; beta4; beta5; beta6; X1; X2; X3; X4; ...
      X5; X6; Y1; Y2; Y3; Y4; Y5; Y6; Fz1; Fz2; Fz3; Fz4; Fz5; ...
      Fz6; u1; u2; u3; u4; u5; u6; v1; v2; v3; v4; v5; v6; ...
      T1; T2; T3; T4; T5; T6; delta1; delta2; delta3; delta4; ...
      delta5; delta6; U1; U2; U3; U4; U5; U6; V1; V2; V3; V4; V5; ...
      V6; dU; dV; dr; ddpsi; dU0; dV0; dU1; dV1; dU2; dV2];

% end mdlDerivatives

%
%=====
% mdlUpdate
% Handle discrete state updates, sample time hits, and major time step

```

```

% requirements.
%=====
%
function sys=mdlUpdate(t,x,u)

sys = [];

% end mdlUpdate

%
%=====
% mdlOutputs
% Return the block outputs.
%=====
%
function sys=mdlOutputs(t,x,u,vd,data)

sys = [t; data];

% end mdlOutputs

%
%=====
% mdlGetTimeOfNextVarHit
% Return the time of the next hit for this block. Note that the result is
% absolute time. Note that this function is only used when you specify a
% variable discrete-time sample time [-2 0] in the sample time array in
% mdlInitializeSizes.
%=====
%
function sys=mdlGetTimeOfNextVarHit(t,x,u)

sampleTime = 1; % Example, set the next hit to be one second later.
sys = t + sampleTime;

% end mdlGetTimeOfNextVarHit

%
%=====
% mdlTerminate
% Perform any end of simulation tasks.
%=====
%
function sys=mdlTerminate(t,x,u)

sys = [];

% end mdlTerminate

Tire Model
function [mux,muy,SR,s,beta] = combinatorMu(vx,vy,vw,xmodel,ymodel,xdata,ydata)

```

```

% COMBINATOR Slip Circle Model for tire combined braking and cornering forces
% [Fx,Fy] = combinator(alpha,SR,tiredata) computes the combined
% braking and cornering forces based on models for pure braking and pure
% cornering.
%
% Inputs:
%   alpha    - tire slip angle in radians
%   SR       - slip ratio (w*R-v*cos(alpha)/(v*cos(alpha)))
%   Fz       - normal force
%   Fxmodel  - Name of function including pure driving/braking tire model
%              with calling syntax Fx = Fxmodel(SR,Fz,varargin)
%   Fymodel  - Name of function including pure cornering tire model
%              with calling syntax Fy = Fymodel(sin(alpha),Fz,varargin)
%   varargin - 2*N optional arguments. Arguments 1:N are passed
%              to Fxmodel, arguments N+1:2*N are passed to Fymodel.
%
% A note on sign conventions (according to SAE standards):
%   sgn(SR) = sgn(Fx)
%   sgn(alpha) = -sgn(Fy)
%
% Reference: Schuring et al. "A Model For Combined Tire Cornering and
%           Braking Forces", SAE Paper 960180, 1996
%
% Magnus Gäfvert 2000
% DICOSMOS
%

SR = (vw-vx)/max(abs(vx),abs(vw));
v = sqrt(vx^2+vy^2);

sinalpha = vy/v;

s = min(sqrt(SR^2 + sinalpha^2),1);
beta = atan2(-sinalpha,SR);

mux0 = abs(feval(xmodel,sign(SR)*s,xdata));
muy0 = abs(feval(ymodel,-sign(sinalpha)*s,ydata));

a0 = 0.5*(mux0 + muy0);
a1 = 0.5*(mux0 - muy0);

mu = a0 + a1*cos(2*beta);

mux = mu*cos(beta);
muy = mu*sin(beta);

function Fx = fxmodel(s,Fz,table)

Fx = interp1(table(:,1),table(:,2),s)*Fz;

```

```
function Fy = fymodel(s,Fz,table)
Fy = interp1(table(:,1),table(:,2),s)*Fz;
```